Journal of Sedimentary Research

Journal of Sedimentary Research, 2019, v. 89, 253–272
Research Article
DOI: http://dx.doi.org/10.2110/jsr.2019.12

MID-CRETACEOUS PALEOPEDOLOGY AND LANDSCAPE RECONSTRUCTION OF THE MID-ATLANTIC U.S. COASTAL PLAIN

JESSE D. THORNBURG,[1,2] KENNETH G. MILLER,[1,3] JAMES V. BROWNING,[1] JAMES D. WRIGHT[1,3]
[1]*Department of Earth and Planetary Sciences, Rutgers University, Piscataway, New Jersey 08854, U.S.A.*
[2]*Department of Earth and Environmental Science, Temple University, Philadelphia, Pennsylvania 19122, U.S.A.*
[3]*Institute of Earth, Ocean and Atmospheric Sciences, Rutgers University, New Brunswick, New Jersey 08901, U.S.A.*

ABSTRACT: **We identified and described Potomac Formation paleosols from three coreholes in New Jersey and Delaware to interpret depositional history and reconstruct regional landscapes during the climatic transition from the Early to the Late Cretaceous. In total, 103 paleosol profiles were described and grouped into five pedotypes (gray, gray-red, purple, red, and brown) ranging in pedogenic maturity from: 1) weakly developed, immature soils formed under poor drainage conditions (gray and gray-red); to 2) moderately developed soils formed under alternating drainage conditions (purple and red); to 3) well-developed, mature soils formed under well-drained conditions (brown). Geochemical and stable-isotope proxies (Ba/Sr and $\delta^{18}O$ on sphaerosiderite) are presented to constrain paleoprecipitation and/or fluvial position and drainage conditions. Potomac Formation Unit I (Barremian to lower Albian) generally displays well-drained, stable landscape conditions upsection, with paleoprecipitation being the main control on development of paleosol type. Potomac Formation Units II (lower Albian to lower Cenomanian) and III (lower Cenomanian) have variable drainage and landscape conditions upsection. Paleoprecipitation exerted a controlling role in the development of paleosol type lower in Unit II, while base-level changes exerted greater influence on landscape conditions upsection into Unit III. Geochemical proxies provide evidence that Unit I was subhumid with episodes of saturation and overall better drainage conditions relative to the overlying units. Units II and III were deposited under more waterlogged conditions, experiencing subhumid to humid conditions, with episodes of enhanced drainage from base-level fall. The use of these proxies is consistent with interpretations made using the macro-features and micro-features of the paleosols and sphaerosiderite $\delta^{18}O$, and emphasizes that the main long-term environmental control on landscape development during this period was initially paleoprecipitation, with progressive influence from base-level changes.**

INTRODUCTION

Paleosols record nonmarine environmental and climatic information during their formation (e.g., Kraus 1999). Soil formation is controlled by physical, chemical, and biological processes, including climate, biota, relief, parent material, and exposure time; these factors influence the morphology, maturity, mineralogy, and chemistry that are preserved in a paleosol (Jenny 1941; Kraus 1999; Retallack 2001). The study of paleosols and, by extension, the processes that led to their formation provide insight into how the landscape of a region evolved. This study identifies and analyzes paleosols and other nonmarine sediments from the mid-Cretaceous Potomac Formation of the New Jersey and Delaware coastal plains (Fig. 1). The goal of this study is to use paleosols to understand the landscape response to variations in ancient climate and sea level.

The mid-Cretaceous has been described through proxy evidence as a greenhouse world with high levels of atmospheric CO_2 (2–10× present CO_2), high average global temperatures ($\sim$ 6°C higher than present), high global sea level, and an enhanced north-to-south atmospheric heat transport that influenced the North American hydrologic cycle (Barron 1983; Wolfe and Upchurch 1987; Spicer and Corfield 1992; Francis and Frakes 1993; White et al. 2001; Royer et al. 2004; Ufnar et al. 2004; Miller et al. 2005; Berner 2006, 2009; Suarez et al. 2011; Haq 2014). Previous studies of palynology and leaf morphology indicate warmth and provide evidence that the Atlantic Coastal Plain was at times a subhumid to subtropical environment (Doyle and Hickey 1976; Hickey and Doyle 1977). The transition from the late Early Cretaceous into early Late Cretaceous (ca. 125–95 Ma) was a period of continental realignment including the early connection between the northern and southern Atlantic basins that created new regional oceanic circulation patterns (Scotese et al. 1988; Poulsen 1999; Norris et al. 2002). Altered circulation patterns are significant because oceanic circulation is one of the major controls on global climate (Poulsen 1999; Norris et al. 2002). Thus, changes in landmass and oceanic geometry likely played a central role in determining climate during this period; this changing climate was recorded in the Potomac Formation sediments.

Most mid-Cretaceous paleoclimate reconstructions have relied on marine isotope records, though a single preserved paleosol provides a wealth of information (albeit time-averaged on the scale of 10^3–10^6 years) regarding conditions during pedogenesis. A vertical succession of preserved paleosols from a single core allows climate trends to be

Published Online: April 2019
 1527-1404/19/089-253

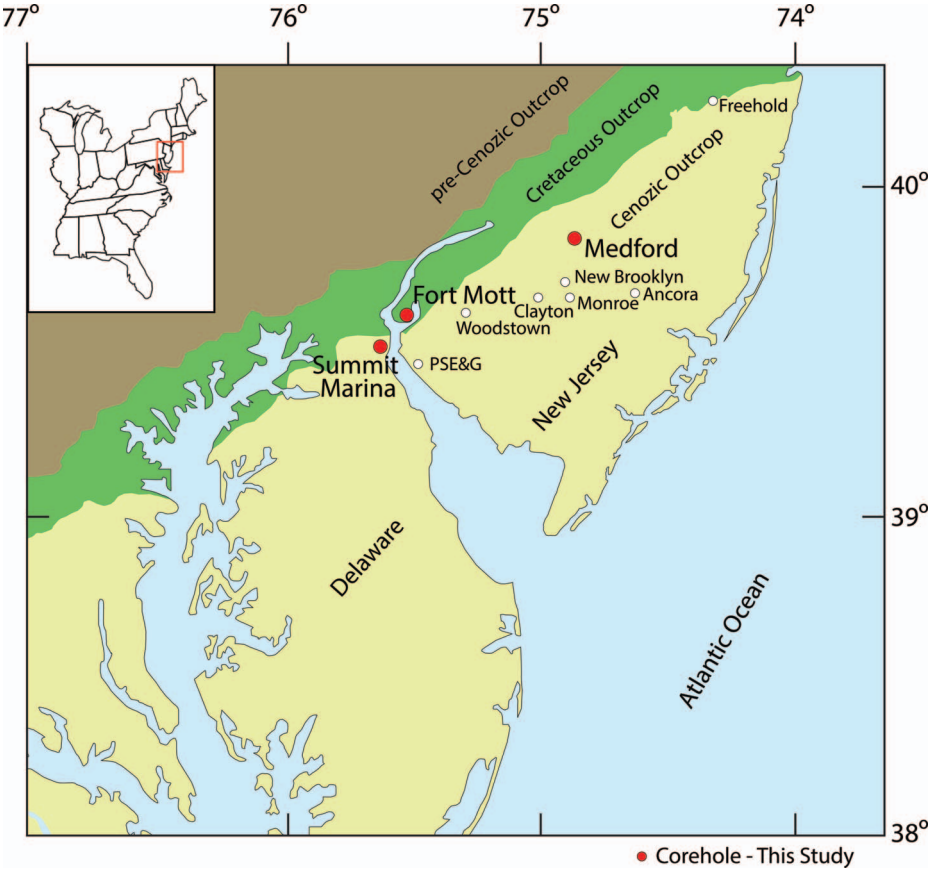

FIG. 1.—Map of the study area.

discerned at a particular location through time. Vertical changes in paleosol profiles provide information on the balance between pedogenesis, sedimentation, and erosion. Weakly developed, stacked, thin profiles form compound paleosols that develop on unstable landscapes with rapid sedimentation. Thick, more mature profiles develop on stable landscapes and form cumulative or composite paleosols. The identification, analysis, and correlation of paleosol profiles can be used to reconstruct the climate and landscape, including changes in base level.

Here, we use a multi-proxy approach to analyze paleosols and their associated sediments. We describe the general morphology of the paleosols to infer the conditions of soil formation and apply a geochemical climofunction and stable-isotope analysis of sphaerosiderite to expand on these interpretations. Each proxy individually has limits and associated uncertainty, but when used together in a multi-proxy approach, they provide a more complete representation of the landscape and its evolution through time. The geochemical analysis measured the ratio of barium to strontium (Ba/Sr), a proxy for the overall drainage conditions during soil formation (Retallack 2001; Sheldon and Tabor 2009). Additionally, stable oxygen-isotope values measured from sphaerosiderite preserve the isotopic signature of meteoric waters during their formation (Ludvigson et al. 1998). Use of these paleoproxies will help discriminate between drainage conditions attributed to changes in precipitation from those attributable to base-level rise and fall.

This study incorporates data from three coreholes recovered from the Atlantic Coastal Plain in New Jersey and Delaware to determine local and regional paleoclimate and base-level changes. Ultimately, the aim of this study is to further enhance understanding of landscape response as global conditions moved towards peak greenhouse conditions.

GEOLOGICAL SETTING

The Fort Mott and Medford, New Jersey, coreholes (Ocean Drilling Program (ODP), Leg 174AX; Fig. 1; Browning et al. 2008; Miller et al. 2005) provide good recovery (79% and 62% respectively) of the Potomac Formation (Fig. 1; Sugarman et al. 2004; Browning et al. 2008; Sugarman et al. 2010). The Summit Marina, Delaware, corehole (drilled in 2009 by the Delaware Geological Survey) provides similar recovery (70%) of the Potomac Formation (Fig. 1). These three sites were chosen to assess changes in local conditions between two closely spaced sites (Summit Marina and Fort Mott) with a more distant site (Medford, 70–85 km along strike) to distinguish those changes that are likely regional in nature.

The Potomac Formation is composed of interbedded fine to medium sands and clay-rich sediments deposited in fluvial and/or deltaic environments during the transition from the Early to the Late Cretaceous (Barremian to early Cenomanian). Updip, the Potomac Formation is found near the base of the coastal-plain section, where it nonconformably overlies crystalline basement rocks, though in downdip sections it is underlain by the Waste Gate Formation (Hansen and Doyle 1982; Olsson et al. 1988; Miller et al. 2017). It is unconformably overlain by lower-delta-plain-estuarine-swamp sediments of the upper Turonian Magothy Formation at Summit Marina and Fort Mott and by the Cenomanian Raritan Formation at Medford (Fig. 2; Browning et al. 2008; Sugarman et al. 2004, 2005, 2010; Zullo 2012). The Potomac Formation has been subdivided into three units, designated Units I, II, and III, each of which is characterized by a succession of medium to fine sand bodies overlain by finer-grained clay and silt units (Sugarman et al. 2004, 2005, 2010; Browning et al. 2008). Accommodation was high during the Albian and Cenomanian due to thermo-flexural subsidence along this margin, allowing thick Potomac Formation deposits to be preserved (Kominz et al. 2008).

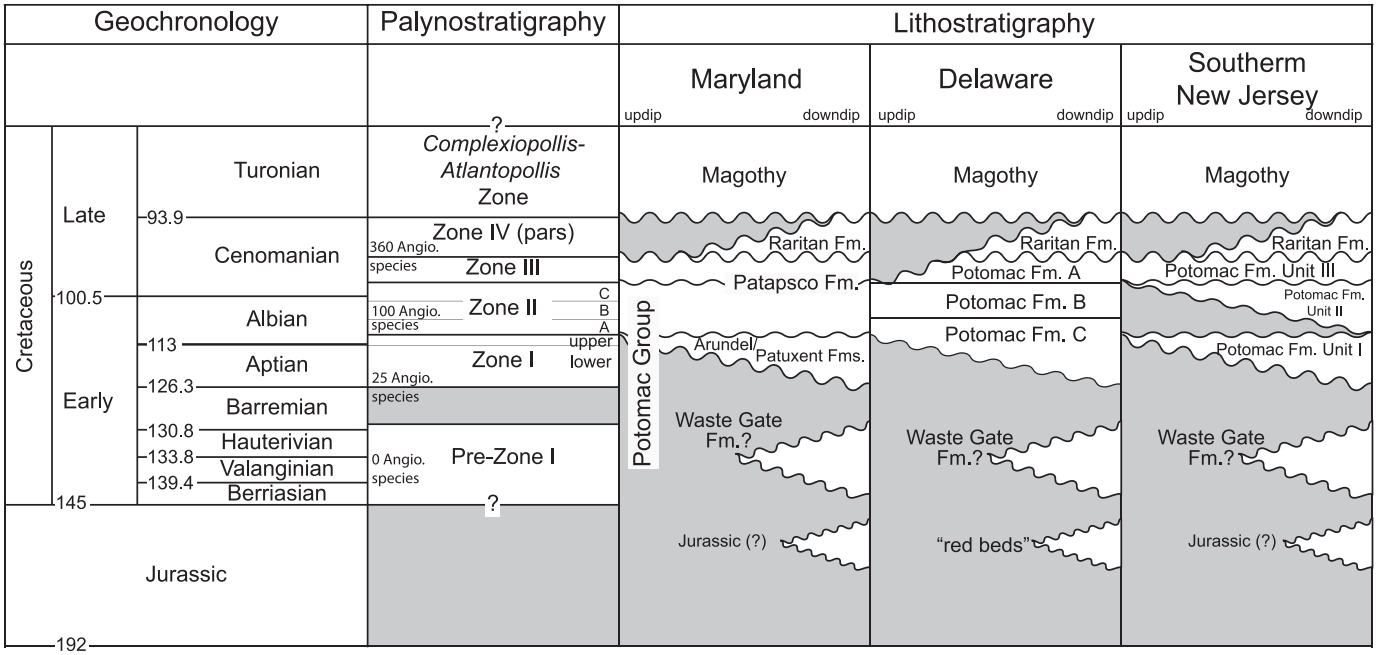

FIG. 2.—Stratigraphic correlation chart for Potomac Formation in New Jersey and Delaware with GTS 2012 and Maryland equivalents (modified from Miller et al. 2017). Angiosperm speciation data are from Lidgard and Crane (1988).

Chronostratigraphic Control

Fossil spores and pollen in the Potomac Formation have been used to develop a palynological zonation that permits interregional correlations (Fig. 2; Brenner 1963; Doyle and Robbins 1977). Three zones have been defined in the Potomac Formation (Zones I, II, and III) with several subzones present in Zone II. These zones are poorly calibrated to the Geological Time Scale (GTS2012, Gradstein et al. 2012) (Fig. 2) and are long in duration (three zones covering ~ 29 Myr; Units I, II, and III are ~ 15, ~ 10, and ~ 4 Myr in duration, respectively). The highest unit, Unit III, is tied to pollen Zone III, assigned by various authors to the early Cenomanian (Doyle and Robbins 1977; Hochuli et al. 2006) and estimated to have an age of ~ 96–100 Ma by correlation to the GTS2012. Unit II is tied to pollen Zone II, assigned to the middle to late Albian (Doyle and Robbins 1977), though it possibly extends to the earliest Cenomanian (Hochuli et al. 2006); its age is estimated as ~ 100–111 Ma (GTS2012). Unit I, the lowermost of the Potomac units, is tied to pollen Zone I and considered Aptian (Hochuli et al. 2006), though it may extend to the Barremian (Doyle and Robbins 1977); it has an estimated age of ~ 111–126 Ma (Fig. 2).

Pollen biostratigraphy does not allow hiatuses to be discerned between the units, but Sugarman et al. (2004, 2005) used erosional breaks associated with facies stacking patterns to infer that each unit was a distinct sequence (*sensu* Mitchum et al. 1977) associated with base-level fall. This implies that hiatuses occurred between deposition of the units, though the hiatuses are within the broad age resolution of pollen biostratigraphy.

METHODS

Core Observations

Macroscopic observations made on paleosol profiles include grain size, ped structure, root structure, color, soil horizonation, hydromorphic, and redoximorphic features (Fig. 3). Color was recorded from dry, unaltered surfaces using the Munsell Soil Color System (Munsell 2000). Horizon designation criteria (Table 1) are modified from modern USDA Soil Taxonomy (Soil Survey Staff 1999). All other field descriptions were made following the National Soil Survey Center field book for describing and sampling soils (Schoeneberger et al. 2002).

Soil micromorphology features were observed on oriented samples, collected and prepared at Temple University using methods outlined by Brewer (1964) (Fig. 4). First, samples were impregnated with epoxy impregnated under vacuum before being dry cut and polished, after which they were mounted to slides, cut, and polished to a thickness of 30 μm. Then, thin-section analysis was completed to detail soil mineralogical and micromorphological features using a Nikon E600 polarizing microscope. Micromorphology features were defined and classified following Brewer (1964) and Fitzpatrick (1993).

Paleosol Classification

All paleosols were described and grouped using a pedotype approach after Retallack (1994, 2001). This method of nongenetic classification focuses on an individual, representative paleosol profile and allows similar profiles to be grouped with this representative paleosol (Retallack 1994). Pedotype grouping is used to group large numbers of paleosol profiles into a classification scheme which is based on lithology and pedogenic features including macromorphology, micromorphology, and clay mineralogy (Fig. 5; Tables 2–4).

Several factors influencing paleosol morphology during formation are considered here: parent material, relief, time, climate, and base level. Parent material is assumed to be consistent at these locations because no large differences in clay mineralogy are observed in analyses done for this study. Relief may play a role in paleosol formation, but given the location of these sites on a low-gradient coastal plain, the role of any significant topographic influence is unlikely. Subtle changes in topography can influence the features of a single soil; these should be negated both by subsequent deposition and the use of multiple paleosols through the section. Landscape stability is also related to time: Alfisols form over longer periods of time on stable landscapes when deposition is slow and episodic; Inceptisols form in short periods of time on relatively unstable

FIG. 3.—Macroscopic paleosol features. **A)** Large, vertical, clay-filled root trace from the A horizon of a Unit I brown type paleosol (Fort Mott, 237.7 m). **B)** Bioturbation with large vertical silt-filled burrows from Unit III (Medford 196.3 m). **C)** Sphaerosiderites concentrated along a root trace in the B horizon of a Unit I red type paleosol (Fort Mott, 233.2 m). **D)** Bioturbation and burrow fills found in Unit III (Fort Mott, 90.1 m). **E)** Large, vertical clay-filled root trace from the B horizon of a Unit III brown type paleosol (Summit Marina, 61.0 m).

surfaces with rapid and unsteady deposition. The time of formation can be quantified to some extent, although genesis can span a time range that is often several orders of magnitude (Retallack 2001; Schaetzl and Anderson 2005). Alfisols (purple, red and brown type) form over 10^3 to 10^6 years, with the more mature red and brown type likely falling towards the higher end of this range (Retallack 2001; Schaetzl and Anderson 2005). Inceptisols (gray and gray-red type) form over 10 to 10^4 years; while generally immature, the paleosols from these sites are mature enough, evidenced from the horizonation features to suggest the upper end of these formation times (Retallack 2001; Schaetzl and Anderson 2005).

Clay Mineralogy

Clay minerals were identified via X-ray diffraction (XRD) pattern analysis using a Rigaku DMAX/B horizontal diffractometer at Temple University and were used to characterize the soils (Table 3). A total of 25 samples were processed for X-ray diffraction (XRD) analysis; this includes a representative sample from every horizon of each pedotype. The clay fraction (< 2 μm) of each sample was prepared by disaggregation of bulk materials by soaking in a bath of deionized and distilled water. Disaggregated samples were spun down by centrifuge at 500 rpm for 12 minutes to separate the clay-size fraction. The clay fraction was removed using a Millipore® Filter Transfer Method prescribed by Moore and Reynolds (1997) and mounted on a glass slide.

Clay-mineral samples were run for analysis at 35 kV and 15 mA using CuKα radiation, scanning from 2 to 40° 2θ at a rate of 1.2° per minute. Data were then processed with Material Data Incorporated's (MDI) Jade 9.1 powder diffraction data analysis acquisition software. Pattern peaks were identified using the International Center for Diffraction Data (ICDD) XRD patterns. A quartz standard was used at the start and finish of each run for quality control, producing characteristic 2θ peaks at 20.8° and 26.6°.

Each sample was analyzed twice: once when untreated and once when glycolated. Glycolated samples were prepared in a desiccator with ethylene glycol for at least 24 hours to remove ambient environmental effects and allow the distinction between swelling and non-swelling clays.

Compaction

Compaction of paleosols was accounted for and determined using the method of Sheldon and Retallack (2001). This method developed the

TABLE 1.—*Criteria for horizon designation (modified Soil Survey Staff 1999).*

Horizon	Criteria
A	When preserved will be uppermost in profile, darkened (from organics) in appearance compared with underlying horizons. Root traces are rare to common. Occasional traces of organic material preserved as charcoal or lignite.
AB	Gradual transition between A and B horizons. Darker in appearance then underlying horizons. Roots will be rare to common. Redoximorphic features that include faint to distinct mottling, drab halo root traces, and iron staining. Occasional evidence of translocated clays. Submillimeter- to millimeter-scale sphaerosiderites are rare to common.
Bt	Horizon defined by the appearance of illuvial clay features. Clay films and clay lamellae are rare to few. Millimeter- to centimeter-scale clay-filled root traces and cracks are rare to common. Redoximorphic features. Faint to distinct mottles. Faint to distinct iron-stained roots and cracks. Submillimeter- to millimeter- scale sphaerosiderites are rare to common.
AC	Transition between A and C horizon, with no B horizon. Faint evidence of redoximorphic features. Rare iron-stained root traces. Submillimeter-scale sphaerosiderites are rare to few. Faint relict bedding is rare.
BC	Transition between B and C horizon. Distinct redoximorphic features. Distinct iron-stained root traces and cracks are few to common. Submillimeter- to millimeter-scale sphaerosiderites are rare to common. Faint relict bedding is rare to common.
C	Parent material with little evidence of pedogenesis. Lighter in appearance than overlying horizons. Relict bedding is common.
Diagnostic Horizons	
Argillic	Subsurface horizon accumulating clay from illuviation, evidenced by clay films, clay lamellae, and clay-filled root traces. Significant increase in clay content from overlying horizons. Thickness greater than 7.5 cm.

following equation to determine total compaction (C) of paleosols from original thickness. The equation is:

$$C = -S_i/\left[\left(F_0/e^{Dk}\right) - 1\right] \quad (1)$$

where S_i represents the initial solidity, F_0 the initial porosity, D the burial depth in km, and k a curve-fitting constant (determined from the relationship between initial and burial porosities (Sheldon and Retallack 2001). Compaction varies based on soil type (e.g., Alfisols and Inceptisols) and uses predetermined values from Sheldon and Retallack (2001) and Soil Survey Staff (1999).

Given the geologic history and stratigraphy, burial depth was assumed to be no deeper than cored depth, as there is no evidence of

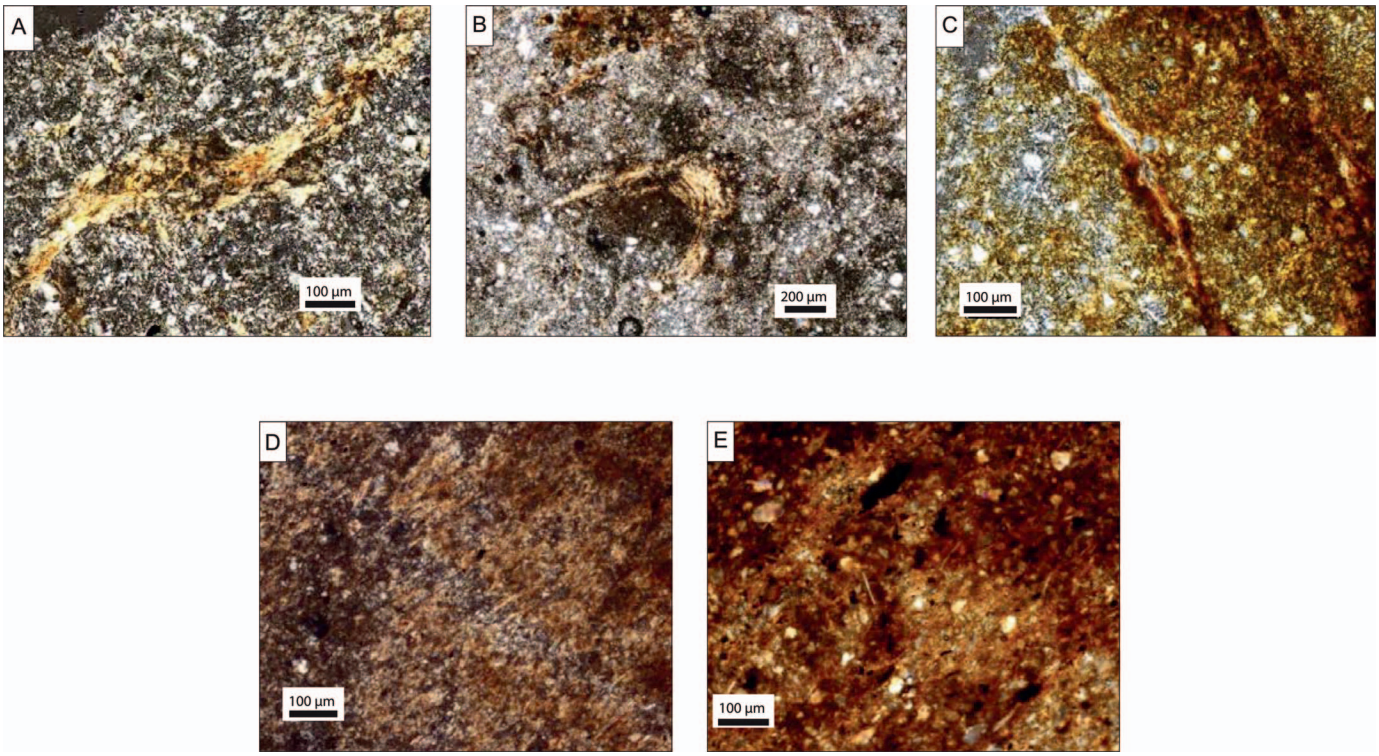

FIG. 4.—Microscopic features of thin sections from cores; all photos are in cross-polarized light. **A**, **B)** Argillans from translocation of clay are common in the B horizon of purple, red, and brown type soils; (Part A, 10×; purple type, Summit Marina, 115.8 m; Part B, 20×; purple type, Medford, 226.2 m). **C)** Iron-staining is common, including these root traces (10×; purple type, Summit Marina, 115.8 m). **D)** Clino-bisepic and Lattisepic clay fabrics are present in gray-red, purple, and red type paleosols, indicating wetting and drying during pedogenesis (10×; red type, Medford, 214.9 m). **E)** Other clay fabrics, including skelsepic, masepic, and random orientations, indicative of more waterlogged conditions present in the gray and gray-red type paleosols; (10×; maesepic to random in a gray type paleosol, Fort Mott, 144.8 m).

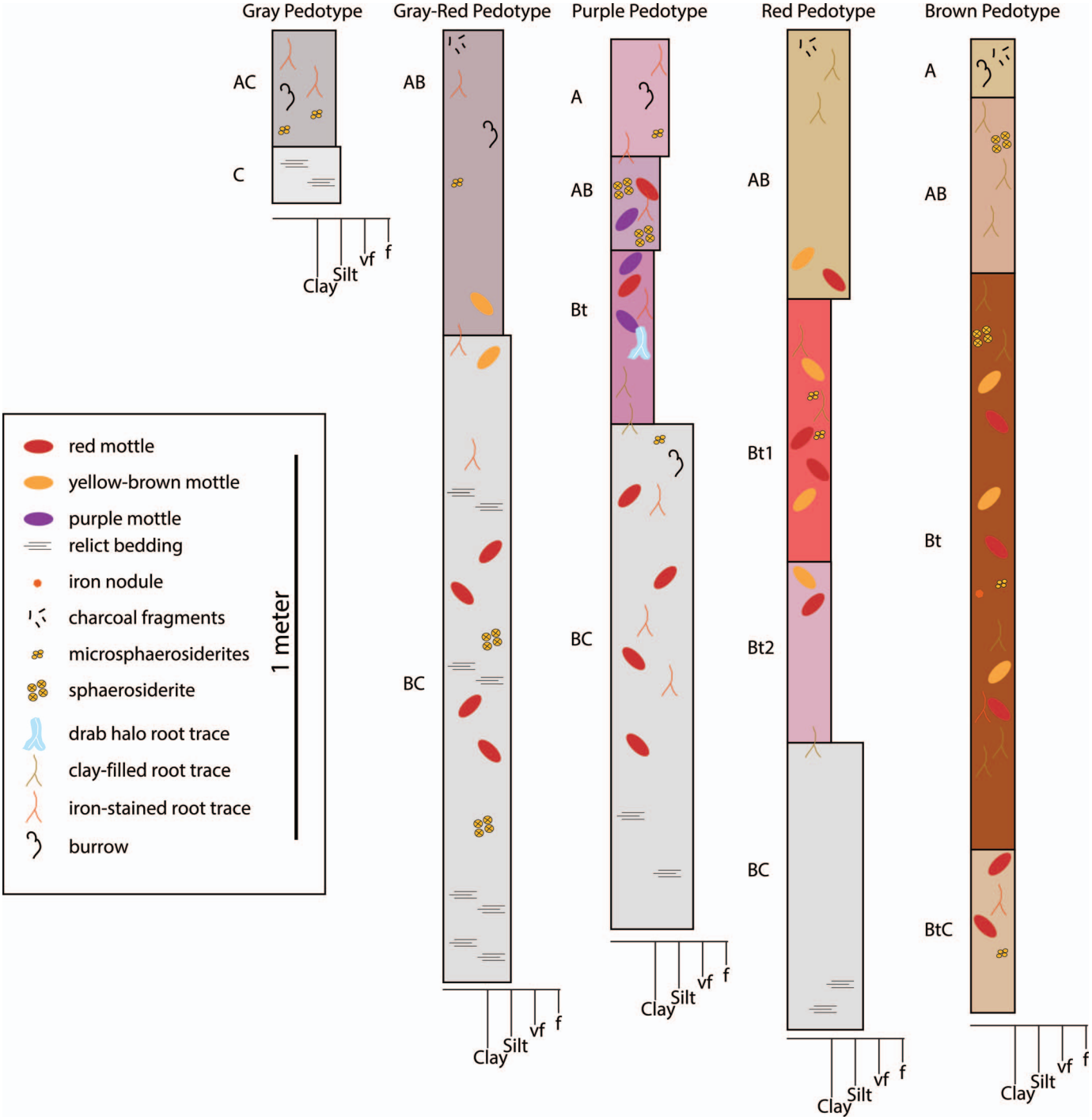

FIG. 5.—Diagrammatic stratigraphic sections for the type paleosols of each representative pedotype.

significant uplift or removal of overburden, with most compaction occurring with the deeper Medford paleosols. Overall, compaction was low and similar at all three sites. Values of compaction from original thickness ranged from 99.7 to 97.8% in the Alfisols to 99.1 to 94.2% in the Inceptisols. As such, compaction was not considered to play a major role in influencing observed paleosol morphology and measured geochemical values.

Bulk Geochemistry

The ratio of barium to strontium (Ba/Sr) of the paleosol profiles was measured to provide proxy records of leaching and drainage conditions (Retallack 2001; Sheldon and Tabor 2009). Bulk samples of 100 g were taken from B horizons (multiple samples for thicker horizons) of 88 samples from 44 profiles for geochemical analysis by X-ray fluorescence

TABLE 2.—*Occurrences and classification of defined pedotypes.*

Pedotype	Occurrences				Classification (Mack et al. 1993)	Classification (USDA 1999)
	Total	Fort Mott	Medford	Summit Marina		
Gray	19	10	2	7	Protosol	Inceptisol
Gray-Red	19	5	4	10	Gleysol	Inceptisol
Purple	23	11	2	10	Gleyed Argillisol	Alfisol
Red	31	22	3	7	Ferric Argillisol	Alfisol
Brown	10	4	1	5	Argillisol	Alfisol
Total		52	12	39		

(XRF) (Table 5). Samples were dried, ground using an agate mortar and pestle to create a uniform size, split using a micro-splitter to avoid density sampling bias, and placed into 32 mm XRF sample cells and covered with 6 μm Mylar® X-Ray film. Three lab standards (SiO_2 180–428; RCRA As, Ba, Cd, Se, Ag 180–436; NCS 73308 180–600) were used as quality control to ensure the proper calibration of the XRF instrument. Precision was routinely between 0.01 and 0.1% of reported values. Major, minor, and trace elements (Ba, Sr, Nb, Rb, Bi, Ar, Se, Pb, W, Zn, Cu, Ni, Co, Fe, Mn, Cr, Va, Ti, Ca, K, Al, P, Si, Cl, Mg) in each sample were measured in triplicate using XRF analysis with a bench-mounted Thermo Niton XL3t-900 in a shielded laboratory stand at Temple University and purged with Helium (He) gas to decrease signal attenuation.

The Ba/Sr ratio provides a proxy for leaching and drainage conditions during pedogenesis (Retallack 2001; Sheldon and Tabor 2009). Lower Ba/Sr values correspond to more saturated, poorly drained conditions and higher values to well-drained conditions. The ranges for each site (Figs. 6–8; Table 5) are given to show variability both through time and across the region. All measured geochemical values are reported by sample depth taken from the B horizon of their respective soil profile (Table 5).

TABLE 3.—*Description of type paleosol horizons for each defined pedotype, including relevant macro- and micromorphological features and dominant clay mineralogy.*

Type	Type Profile and Depth	Horizon, Boundary, and Depth (cm)	Color	Subordinate Color(s)	Macro-morphology	Micro-morphology	Dominant < 2 μm clay mineralogy
Gray	Fort Mott 50.29 m (165 ft)	AC 0–30.5 Diffuse C 30.5–48.8	10YR 6/6 N7	10R 4/6	Fairly featureless Few, faint root traces	Clino-Bisepic to Masepic clay fabrics	Kaolinite Illite Quartz
Gray-Red	Fort Mott 54.86 m (180 ft)	AB 0–70.1 Gradual BC 70.1–243.8	10YR 5/4 5R 3/4	10R 7/4 10YR 8/2 5P 6/2 N8	Few faint to distinct fine to medium mottles; light brown to light red Redoximorphic features including: zones of iron concentrations	Iron Staining Clino-Bisepic to Masepic clay fabrics	Kaolinite Illite Quartz
Purple	Summit Marina 128.02 m (420 ft)	A 0–30.5 Clear/Wavy to Irregular AB 30.5–54.9 Clear/Smooth Bt 54.9–100.6 Gradual/Wavy BC 100.6–231.7	5Y 8/1 5Y 8/1 10R 4/6 10R 4/6	2.5Y 8/2 10R 4/6 10R 4/6 10R 7/3 10R 7/3 10R 7/4 10R 4/8 5Y 4/3	Many prominent coarse to extremely coarse mottles; red and purple in color Many iron-stained root traces Sphaerosiderites present	Clino-Bisepic and lattisepic clay fabric Iron Staining	Kaolinite Illite Quartz Goethite
Red	Fort Mott 70.10 m (230 ft)	AB 0–45.7 Clear/Wavy Bt1 45.7–112.8 Gradual/Smooth Bt2 112.8–271.3 Gradual/Smooth BC 271.3–329.2	5Y 6/1 5Y 8/1 5R 4/6 10YR 8/2	10YR 7/4 5Y 6/1 5R 3/4 5P 4/2	Many prominent coarse to extremely coarse mottles; red in color Many iron-stained and clay-filled root traces Sphaerosiderites present	Clino-Bisepic and lattisepic clay fabric Translocated clay	Kaolinite Illite Quartz Goethite
Brown	Medford 259.08 m (850 ft)	AB 0–45.7 Clear/Smooth Bt 45.7–289.6 Clear to Gradual CB 289.6–332.2	2.5YR 4/6 2.5YR 4/6 2.5YR 4/6	10YR 8/3 10R 4/6 5Y 6/1 10YR 7/1 10R 4/6	Many prominent coarse to extremely coarse mottles; brown and red in color Many clay-filled root traces	Clino-Bisepic clay fabric Translocated clays	Kaolinite Goethite

Stable-Isotope Geochemistry

This study uses stable-isotope data from sphaerosiderite nodules found in paleosol profiles. Sphaerosiderites form under pedogenic conditions and show utility as a paleogroundwater and paleoprecipitation proxy (Cerling 1984; Mora et al. 1996; Ludvigson et al. 1998, 2013; Ufnar et al. 2001, 2002, 2004, 2008; White et al. 2001, 2005; Dworkin et al. 2005; Nordt et al. 2006; Suarez et al. 2011). Sphaerosiderite is found as millimeter to submillimeter scale spherical iron carbonate nodules consisting of siderite ($FeCO_3$). These nodules form in modern soils under reduced, saturated conditions (Stoops 1983; Landuyt 1990; Driese et al. 2010; Ludvigson et al. 2013). Sphaerosiderites preserve oxygen-isotope values that reflect the composition of groundwater and by extension, the meteoric water during their formation, although the potential for mixing of groundwater due to marine incursion needs to be considered (Ludvigson et al. 1998, 2013; White et al. 2005). Thus, isotopic $\delta^{18}O$ data from sphaerosiderites act as a proxy for paleohydrologic conditions (specifically paleogroundwater and paleoprecipitation) during their formation (Ludvigson et al. 1998, 2013; Ufnar et al. 2002; White et al. 2005; Suarez et al. 2011). When taken from a single horizon, sphaerosiderite isotopic values produce relatively invariant $\delta^{18}O$ values and varying $\delta^{13}C$ values, defining a meteoric sphaerosiderite line (*sensu* Ludvigson et al. 1998), with the $\delta^{18}O$ values reflecting groundwater $\delta^{18}O$ values (White et al. 2001, 2005).

Several sphaerosiderite horizons were sampled from paleosol profiles to evaluate the influence of paleoprecipitation through time at all three coreholes. Multiple samples were taken for isotopic and thin section analysis. In total, 31 horizons were sampled: 17 from Fort Mott, 8 from Summit Marina, and 6 from Medford (Table 6). Samples for thin section were collected, epoxy-mounted to a glass slide, and polished to analyze for potential oxidation or late-diagenetic alteration (Fig. 9). Four representative horizons were analyzed with XRD to confirm the presence of siderite and to discount any potential contamination from other carbonates. These horizons were chosen because the siderites have a range of rim oxidation alteration (Fig. 9). No contaminating phases of carbonate minerals were observed (see Supplemental Material).

Isotope analyses were carried out at Rutgers University on a Micromass Optima mass spectrometer. Sphaerosiderites were separated from matrix, washed, and crushed with an agate mortar and pestle to obtain 100–300 micrograms. When necessary, multiple sphaerosiderites from a single horizon were combined to attain enough material for analysis. Each horizon was sampled separately and multiple (2–7) times based on the availability of material. Powdered samples were placed in reaction vials and loaded using an automated Multiprep device attached to the device. Samples were reacted for 10 minutes in phosphoric acid at 90°C; the evolved CO_2 was then collected in a liquid-nitrogen cold finger. Stable-isotope values are reported versus Vienna Pee Dee Belemnite (VPDB) through the analysis of an in-house laboratory standard (RGF1). This standard is routinely calibrated to NBS-19, and precision on the standards is 0.05 and 0.08 for $\delta^{13}C$ and $\delta^{18}O$, respectively. The averaged results of each horizon are presented below; the results of each individual analysis are presented in supplemental Table 1.

The oxygen-isotope composition of meteoric waters (reported as Vienna Standard Mean Ocean Water (VSMOW)) is determined from sphaerosiderites using a temperature-dependent fractionation factor. This correction accounts for temperature-dependent fractionation between siderite and phosphoric acid using the derived equation of van Dijk et al. (2018).

The fractionation factor equation is described as follows:

$$10^3 \ln \alpha = 19.67 \pm 0.42\left(10^3/T_K\right) - 36.27 \pm 1.34 \quad (2)$$

where α is the siderite-water ^{18}O isotope fractionation factor and T_K is the temperature of precipitation in kelvins. Paleotemperature is needed to determine the isotopic composition of meteoric water in these fractionation equations, because the range of $\delta^{18}O$ VSMOW values relate directly to temperature (Fig. 10). Temperature was determined using a zonal gradient developed using Cretaceous leaf physiognomy by Wolfe and Upchurch (1987), confirmed by Spicer and Corfield (1992), and also subsequently reported by Ufnar et al. (2002) and Suarez et al. (2011).

This temperature gradient is given as the equation

$$T = 30.25 - 0.2025 * \varphi - 0.0006 * \varphi^2 \quad (3)$$

where T is the temperature and φ is the paleolatitude. Based on reconstructions of Barron (1987) and Hay et al. (1999), a paleolatitude of 30°N was used to approximate the mean annual temperature of ~ 24°C during sphaerosiderite formation.

RESULTS

Paleosols

A total of 103 paleosols were identified and described across the three sites. At Fort Mott, 52 total profiles were identified: 19 in Unit III, 12 in Unit II, 1 in Unit I/II and 20 in Unit I (Fig. 6). At Summit Marina, 39 total profiles were identified: 15 in Unit III and 24 in Unit II (Fig. 7). At Medford, 12 total profiles were identified: 6 in Unit III and 6 in Unit II (Fig. 8).

Five pedotypes were defined from the Potomac Formation: gray, gray-red, purple, red, and brown. The gray type and gray-red type of paleosols are Protosols, similar to modern Inceptisols, with weak horizon development (A and C with occasional development of a B horizon in the gray-red type) reflecting rapid formation from parent material (Tables 2–4; Mack et al. 1993; Retallack 2001; Soil Survey Staff 1999). The purple, red, and brown type paleosols are Argillisols, similar to modern Alfisols that formed over a longer period of time (Tables 2–4; Mack et al. 1993; Retallack 2001; Soil Survey Staff 1999). All paleosol profiles are reported in Supplemental Table 2.

The gray type of paleosol was identified in cores at all three sites (Fort Mott (n = 10), Summit Marina (n = 7), and Medford (n = 2)). This pedotype is the least mature with little pedogenic modification, including initial weak horizonation, and few, faint to distinct, small (mm-scale) mottles (Fig. 5; Table 4). This weakly developed soil displays features of waterlogged, poor-drainage conditions including drab halo root traces, low chroma values (ranges between 0 and 4), skelsepic and masepic clay fabrics, iron nodules, and microsphaerosiderites in several of the profiles (Figs. 3–5).

The gray-red type of paleosol has increased pedogenic modification relative to the gray type, and with better development of horizons, including the development of a BC horizon, is identified at all three sites (Summit Marina (n = 10), Fort Mott (n = 5), and Medford (n = 4)). However, this type is still weakly developed overall (Fig. 5; Table 4). Pedogenic features include higher chroma values (4–6) in the upper horizons relative to the lower horizons (1–4), suggesting drying in the upper horizons after a period of saturation. This is supported by bisepic clay fabrics and mottling with translocated iron (stained root traces and cracks) as well as sphaerosiderites that are found in the lower horizons of several profiles of this type (Figs. 3–5).

The purple type exhibits features of mature pedogenic development with distinct horizons including an argillic horizon (Summit Marina (n = 10), Fort Mott (n = 11), and Medford (n = 2)). However, pedogenic development was either inhibited or ceased at times due to saturated conditions, suggesting the possibility of seasonal wet–dry cycles during formation (Fig. 5; Table 4). Waterlogged conditions are evidenced by lower chroma values (2–4), fine root mats, and drab halo root traces. However, the presence of many, large (cm-scale) mottles, clay skins, sphaerosiderites, iron staining, and bisepic clay fabrics attests to breaks in saturated conditions (Figs. 3–5). The purple type is similar to modern Alfisols formed in semiarid to humid areas, usually under forest cover.

TABLE 4.—*Description of diagnostic features for the defined pedotypes.*

Pedotype	Horizonation	Development/Maturity	Rooting	Other
Gray	Diffuse to Absent	Very Weak	• Small, fine • Occasional drab halos	
Gray-Red	Diffuse to Gradual	Weak to Moderate	• Small, vertical • Clay-filled • Fe-stained	• Occasional sphaerosiderite • Few to common mottles
Purple	Clear	Moderate	• Fine, horizontal mats • Fe-stained • Drab halos	• Many, coarse mottles • Common Fe staining • Common Sphaerosiderites
Red	Clear	Moderate to Well	• Small, vertical • Clay-filled	• Common fine to medium mottles • Occasional Fe staining • Occasional Sphaerosiderites
Brown	Clear	Moderate to Well	• Small, vertical • Clay-filled	• Many, medium to coarse mottles

The red type of paleosols are mature (even more so than the purple type) with well-developed horizons, including an argillic horizon, and moderate chroma values (3–6) (Fort Mott (n = 22), Summit Marina (n = 7) and Medford (n = 3)) (Fig. 5; Table 4). Features suggest enhanced drainage with occasional periods of waterlogged conditions. Clay-filled root traces and iron staining are found along root traces and throughout cracks; sphaerosiderites are also present in several profiles. Many large (cm-scale) mottles are present. Argillans and bisepic clay fabrics are observed in thin section (Figs. 3–5).

The brown type of paleosol is the most mature and well-developed paleosol, with distinct horizonation, an argillic horizon, and translocated clay features (Fort Mott (n = 4), Summit Marina (n = 5) and Medford (n = 1)). The latter include long (cm-scale) vertical roots that are preserved through clay-infilling, indicating well-drained conditions (Fig. 5; Table 4). Higher chroma values (4–6) are found throughout the profile as well as many large (cm-scale) red and brown mottles. Rare iron staining and sphaerosiderites are found in some profiles (Figs. 3–5).

The occurrences of pedotypes can be placed in a stratigraphic context. The gray and gray-red types, forming under poorly drained, waterlogged conditions, are best developed in Units II and III at all three sites (25–63% of all profiles identified in each unit). Gray type profiles at Fort Mott account for 3 of 12 identified profiles in Unit II and 7 of 19 in Unit III and again are grouped in the middle and top of the unit. Gray-red account for 3 of 12 in Unit II and 5 of 19 in Unit III grouped near the top of the unit. At Summit Marina, gray type profiles account for 2 of 24 (Unit II) and 5 of 15 (Unit III), grouped mainly in the lower and middle part of the unit. Gray-red accounts for 5 of 24 Unit II profiles and 4 of 15 Unit III profiles, grouped in the middle to upper part of the unit. At Medford, gray profiles

TABLE 5.—*Calculated geochemical proxy values; lower Ba/Sr values correspond to decreased leaching, higher values correspond to increased leaching. (FM, Fort Mott; SM, Summit Marina; MT, Medford).*

Sample Depth (m)	Soil ID	Ba/Sr	Sample Depth (m)	Soil ID	Ba/Sr	Sample Depth (m)	Soil ID	Ba/Sr
34.3	SM110	3.9	52.7	FM170	2.5	210.4	MT690	1.9
49.6	SM160	5.5	55.7	FM180	2.2	214.5	MT705	2.6
50.9	SM165	5.4	58.8	FM190	3.8	226.6	MT742	1.4
51.7	SM170	2.2	63.5	FM210	2.1	228.3	MT749	2.9
62.4	SM200	3.8	75.3	FM250	4.2	240.8	MT790	1.7
105.8	SM345	7.2	80.4	FM260	2.1	242.6	MT795	2.3
111.9	SM365	3.3	83.5	FM270	3.0	245.7	MT800	1.6
117.0	SM385	4.2	96.5	FM315	2.5	260.3	MT850	3.4
128.8	SM420	2.5	112.2	FM370	1.7			
134.5	SM440	4.4	116.4	FM380	2.0			
136.5	SM445	3.5	120.4	FM395	1.7			
140.6	SM460	2.1	126.6	FM415	1.8			
146.7	SM480	2.5	155.6	FM510	1.8			
			157.8	FM520	2.8			
			162.3	FM530	2.9			
			165.5	FM540	1.3			
			198.3	FM650	1.0			
			213.4	FM700	2.0			
			214.8	FM705	1.0			
			224.0	FM730	6.0			
			228.6	FM750	5.4			
			232.9	FM760	1.4			
			234.9	FM770	6.4			
			239.3	FM780	5.9			

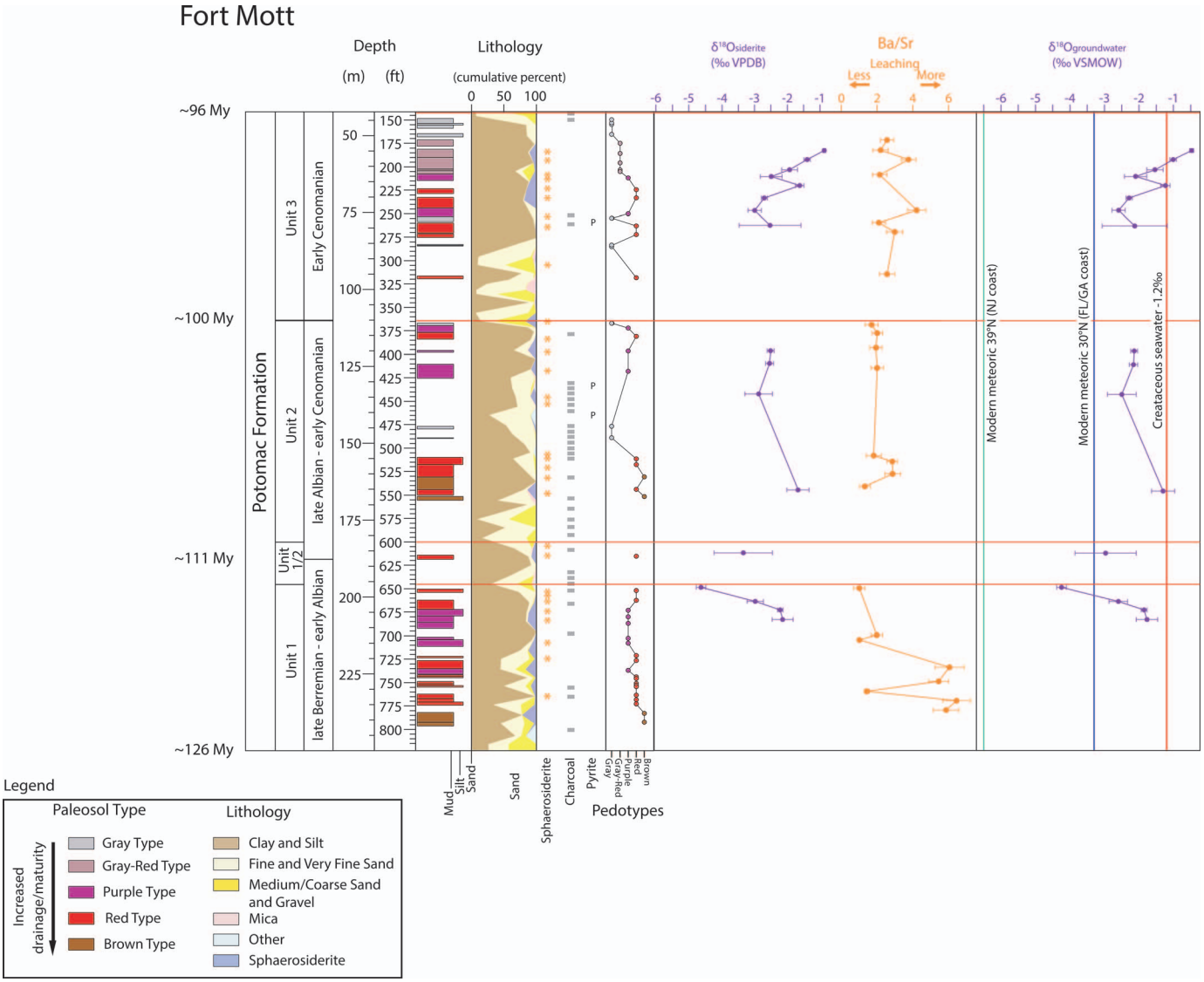

FIG. 6.—Fort Mott—cumulative lithology, gamma, resistivity, paleosol pedotype, stable oxygen values from pedogenic sphaerosiderites, barium/strontium ratio distribution, and calculated groundwater oxygen isotope values for the Potomac Formation. Cretaceous seawater and modern meteoric value lines are given for comparison with calculated values.

account for 1 of 6 in both Units II and III, and gray-red for 2 of 6 in both Units II and III.

The purple and red Types of paleosol provide evidence of land stability with enhanced drainage. These Types are identified in Unit I at Fort Mott (90% of identified unit profiles) and in Units II and III at Summit Marina, Fort Mott, and Medford (33–58% of all profiles identified in each unit). At Fort Mott, purple type paleosols account for 6 of 20 profiles in Unit I, 3 of 12 profiles in Unit II, and 2 of 19 profiles in Unit III, grouped typically in the middle or upper part of the units. Red type paleosols account for 12 of 20 profiles in Unit I, 1 of 1 in Unit I/II, 4 of 12 profiles in Unit II, and 5 of 19 profiles in Unit III. At Summit Marina, purple type paleosols account for 8 of 24 profiles in Unit II, and 3 of 15 profiles in Unit III. Red type paleosols account for 5 of 24 profiles in Unit II, and 2 of 15 profiles in Unit III. At Medford, purple type paleosols account for 1 of 6 profiles in both Units II and III, and red account for 1 of 6 and 2 of 6 in Units II and III, respectively.

The brown type, indicative of the relatively greatest stability and best drainage, is identified in Unit I at Fort Mott (10%), in Unit II at Summit Marina, Fort Mott, and Medford (16% of identified unit profiles), and in Unit III at Summit Marina (6% of identified unit profiles). At Fort Mott, brown type paleosols are identified in 2 of 20 profiles in Unit I, 2 of 12 in Unit II. At Summit Marina, brown type paleosols are identified in 4 of 24 and 1 of 15 in Units II and III, respectively. At Medford, brown type paleosols are identified in 1 of 6 profiles in Unit II.

The classic application of paleosols is to interpret paleoenvironmental significance and landscape evolution (Kraus 1999). However, we show below that the paleosol stacking patterns can also be used to aid in correlations among sites.

Clay Mineralogy

Kaolinite is the major clay mineral present in all 25 samples, with lesser amounts of smectite and illite. The presence of smectite is supported by shrink–swell features in some of the paleosol profiles. The illite is mostly allogenic, having formed elsewhere and deposited only at these sites, although it is possible that some smectite underwent illitization during

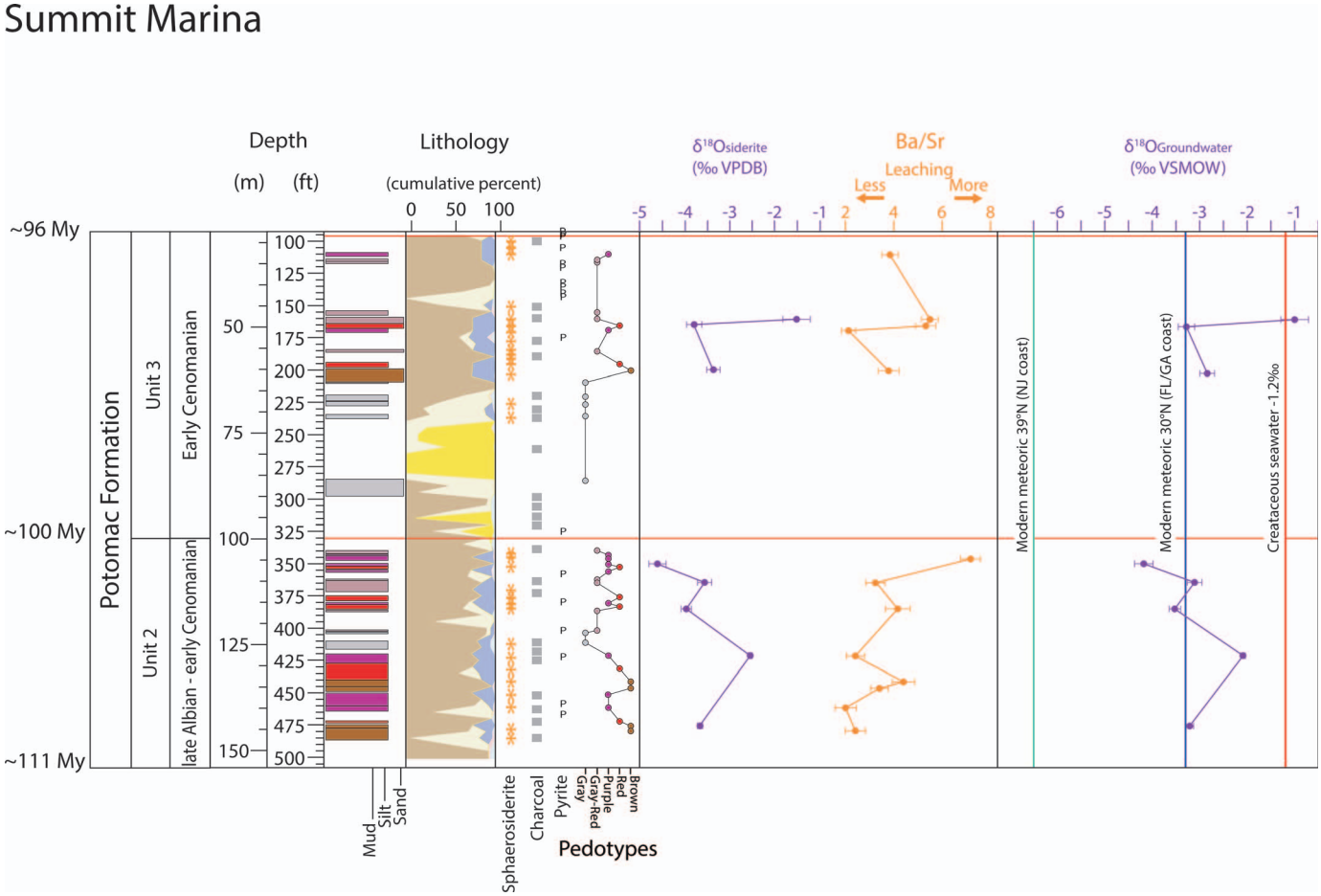

FIG. 7.—Summit Marina—cumulative lithology, gamma, resistivity, paleosol pedotype, stable-oxygen-isotope values from pedogenic sphaerosiderites, Barium/Strontium ratio distribution, and calculated groundwater oxygen-isotope values for the Potomac Formation. Cretaceous seawater and modern meteoric value lines are given for comparison with calculated values.

pedogenesis for in-situ formation. However, these soils did not reach burial depths and pressures great enough to transform most of the smectite into illite. Quartz and goethite also are present in several of the paleosols in the clay-size fraction.

Correlation

Thick intervals of sand found at the bases of Units II and III have previously been shown to be laterally traceable on a regional scale (Sugarman et al. 2005; Miller et al. 2017; Thornburg 2016) and therefore offer correlatable surfaces. Distinguishing the depositional environment provides further support for correlation. The environment of deposition of the basal sands is uncertain, for there remains a question of distinguishing discontinuous facies of an anastomosing system deposited on a delta plain (e.g., Makaske 2001) from more laterally continuous sands deposited in a delta front. The lack of marine or marginal marine fossils in our cores precludes a definitive interpretation of a delta-front facies. The basal sands of Unit II and III can be traced up to 60 km along strike, suggesting a widespread environment such as a delta front (Sugarman et al. 2005; Miller et al. 2017); although individual sands beds are discontinuous, at least in updip sites, like the cores examined here (Benson and McLaughlin 2006).

Previous studies by Sugarman et al. (2005) and Thornburg (2016) have shown that Potomac Units I through III correlate widely; the units themselves span broad ranges of geologic time. We confirm previous unit correlations and attempt to correlate sites at the sub-unit scale in the Potomac Formation. Surfaces in the units should provide a higher resolution of correlation across the Potomac Formation.

Unit I.—Only the Fort Mott and Medford coreholes reach Unit I of the Potomac Formation and Unit I is assigned to pollen Zone I (?Barremian to Aptian) (Figs. 6, 8; Sugarman et al. 2004, 2010). No paleosols are present in Unit I at the Medford site (Fig. 7); sands and gravels dominate this section, which are interpreted as a braided fluvial environment based on the coarse-grained gravel and sand lithology (Sugarman et al. 2010). This contrasts with the more typically medium to fine sand and silt lithologies at Fort Mott (Fig. 6), where Unit I is interpreted to represent anastomosing fluvial environments (Sugarman et al. 2005). Along strike, Unit I has both blocky gamma-log patterns interpreted as braided deposits (New Brooklyn and Woodstown; Fig. 1; Miller et al. 2017) and lower gamma-log values interpreted as anastomosing deposits (Monroe, Clayton, and PSE&G; Fig. 1; Miller et al. 2017), documenting abrupt facies changes during the initial deposition of the Potomac Formation. Direct correlation between Fort Mott and Medford is broad; the unit designation is based on general lithology, though this is supported by pollen biostratigraphic correlation to Zone I (Sugarman et al. 2005, 2010; Miller et al. 2017).

Unit II.—The basal sands of Unit II at Fort Mott and Medford have been interpreted by Sugarman et al. (2004, 2005, 2010) and Miller et al. (2017) as forming on an anastomosing fluvial landscape. The Summit

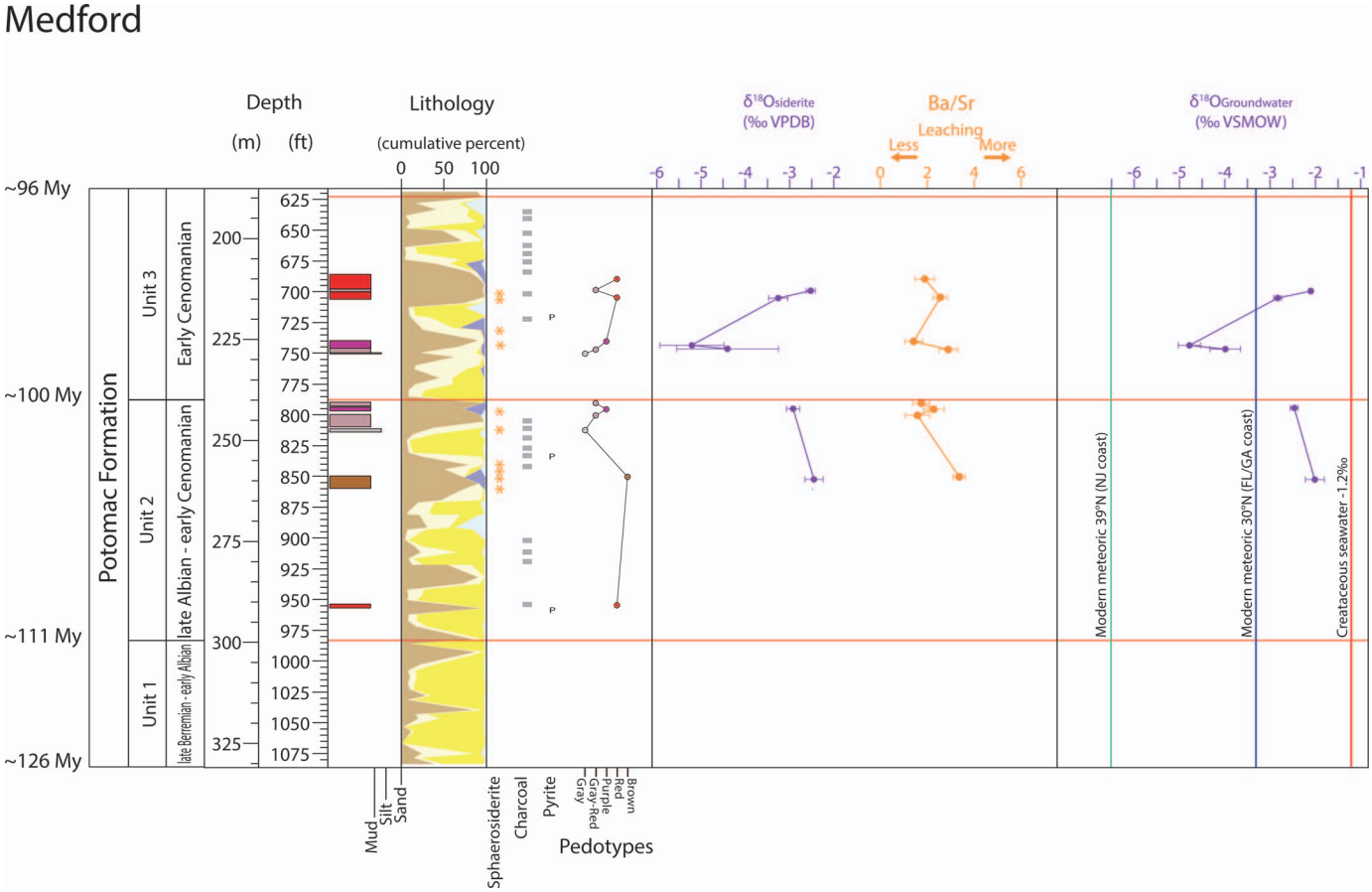

FIG. 8.—Medford—cumulative lithology, gamma, resistivity, paleosol pedotype, stable-oxygen-isotope values from pedogenic sphaerosiderites, barium/strontium ratio distribution, and calculated groundwater oxygen-isotope values for the Potomac Formation. Cretaceous seawater and modern meteoric value lines are given for comparison with calculated values.

Marina borehole reaches into Unit II but not to the base of the sequence (Fig. 7). However, given the depth, proximity, and grain characteristics, the sands (although not as clean, containing interbeds of silt and clay) at the bottom of the Summit Marina hole are here interpreted as roughly correlatable to those sands at the base of Unit II at Fort Mott (Fig. 11).

The paleosols above the sand interval are also interpreted as correlatable among the three core sites. Stability and drainage are evidenced at the unit base by brown, red, and purple paleosols at Summit Marina and brown and red paleosols at Fort Mott. At Medford, a possible correlation to this interval at Fort Mott and Summit Marina is given by a single brown paleosol profile found in the middle of this unit. Upsection from this, at all three sites, an interval of heterolithic sands with poorly developed and waterlogged paleosols offers a correlatable interval.

The extent to which an anastomosing system is separate from, occurs on, or overlaps with a deltaic system is ambiguous (Makaske 2001 and references therein). Thus, the correlation of individual sand beds is tenuous, although the basal sand body of Unit II is regionally correlatable above the basal unconformity (Sugarman et al. 2005; Miller et al. 2017). Regardless, the paleosols offer evidence of precipitation–evaporation and base-level conditions of the landscape on which they formed, aiding in the correlation between sites.

Unit III.—The Unit II–III boundary is interpreted at the base of a sand body at all three sites: 100.6–94.5 m at Summit Marina, 110.8–97.7 m at Fort Mott, and 239.8–231.9 m at Medford (Figs. 6–8). As discussed above, we favor interpretation of these laterally continuous sand zones as delta front deposits, including numerous occurrences of pyrite and wood and/or charcoal material (Figs. 6–8). The deposition of these sands was followed by a period of soil formation at all three locations. This includes a weakly developed, compound gray paleosol at Summit Marina and a red paleosol at Fort Mott indicative of a period of relative stability with increasing drainage. At Medford, purple, gray-red, and gray compound profiles are found to have formed under varying levels of saturation. A second body of sands overlies these paleosols at all three sites: 86.6–72.5 m at Summit Marina, 96.0–88.4 m at Fort Mott, and 220.0–216.4 m at Medford (Figs. 6–8). At all three sites, this sand body lies above an interpreted erosional contact with scattered pyrite, organic matter, burrows, and cross-bedding, and may reflect a higher-order sequence boundary.

The upper sands at Fort Mott and Medford in Unit III are similar to the basal sands in Unit II, are apparently laterally continuous, and roughly correlatable (Fig. 12). These sand bodies are interpreted as channel fill from an anastomosing fluvial system. Avulsion is a likely explanation for the deposition of these heterolithic sands, silts, and clays with the associated weakly developed gray and gray-red paleosols. However, this explanation is more problematic for the purple paleosol at Medford and red paleosol at Fort Mott found in this sand body, given the greater degree of development of these paleosols. Nevertheless, avulsion events can result in the fluvial channel at each site becoming more distal, enhancing drainage, and allowing soils a longer time to form on this increasingly stable landscape.

TABLE 6.—*Stable-oxygen-isotope values from pedogenic siderites, values represent averaged measurements from single horizons. Measured $\delta^{13}C_{siderite}$ and $\delta^{18}O_{siderite}$ values are reported in ‰ VPDB. Groundwater $\delta^{18}O$groundwater values are calculated using the fractionation factor of van Dijk et al. (2018) and reported in ‰ VSMOW. (FM, Fort Mott; SM, Summit Marina; MT, Medford).*

Sample Depth (m)	Soil ID	$\delta^{13}C_{siderite}$	±	$\delta^{18}O_{siderite}$	±	$\delta^{18}Og_{roundwater}$	±
55.8	FM180	–22.23	1.35	–0.88	0.04	–0.4	0.04
58.8	FM190	–15.12	0.19	–1.41	0.09	–1.0	0.09
61.9	FM200	–27.03	9.02	–1.94	0.24	–1.5	0.24
64.0	FM210	–21.51	4.84	–2.50	0.33	–2.1	0.33
67.1	FM220	–28.57	1.17	–1.64	0.13	–1.2	0.13
71.0	FM230	–25.10	0.05	–2.71	0.09	–2.3	0.09
75.2	FM250	–15.59	0.41	–3.00	0.20	–2.6	0.20
79.9	FM260	–14.28	0.38	–2.54	0.94	–2.1	0.94
120.7	FM395	–18.84	0.10	–2.54	0.10	–2.1	0.10
125.0	FM415	–20.74	0.09	–2.57	0.12	–2.1	0.12
134.7	FM442	–7.91	0.22	–2.91	0.42	–2.5	0.42
166.3	FM540	–16.39	0.02	–1.70	0.34	–1.3	0.34
186.2	FM615	–11.27	0.20	–3.38	0.89	–2.9	0.89
197.8	FM650	–12.50	0.19	–4.67	0.14	–4.2	0.14
202.1	FM660	–18.05	1.55	–3.01	0.27	–2.6	0.27
205.1	FM670	–16.97	0.73	–2.25	0.08	–1.8	0.08
208.2	FM680	–13.87	0.40	–2.18	0.32	–1.7	0.32
48.9	SM160	–15.63	0.12	–1.42	0.30	–1.0	0.30
50.5	SM165	–17.63	0.16	–3.70	0.17	–3.3	0.17
61.9	SM200	–18.56	0.02	–3.26	0.14	–2.8	0.14
106.7	SM350	–19.80	0.24	–4.59	0.19	–4.2	0.19
112.5	SM365	–18.77	0.08	–3.53	0.16	–3.1	0.16
116.7	SM385	–17.37	0.05	–3.94	0.11	–3.5	0.11
128.2	SM420	–20.93	0.03	–2.54	0.05	–2.1	0.05
145.0	SM475	–19.22	0.07	–3.65	0.06	–3.2	0.06
213.4	MT700	–18.33	2.43	–2.53	0.11	–2.1	0.11
214.9	MT705	–12.34	0.55	–3.26	0.22	–2.8	0.22
226.8	MT742	–14.59	0.45	–5.21	0.7	–4.78	0.7
227.7	MT749	–14.47	0.26	–4.41	1.1	–3.97	1.1
242.2	MT795	–15.46	0.06	–2.91	0.15	–2.5	0.15
259.9	MT850	–15.64	0.24	–2.45	0.20	–2.02	0.20

Paleosol Packages.—At all of the study sites there are alternating series of paleosols that group into packages of mature, enhanced drainage paleosols (brown and red) and immature, diminished drainage paleosols (purple, gray-red, and gray). These packages contain multiple stacked paleosol profiles, and their resulting stacking pattern offers a way to correlate between these sites.

At Summit Marina, paleosols at the base of Unit II are mainly mature brown and red profiles indicative of landscape stability. Overlying this package is a group of purple, gray-red, and gray paleosols, indicative of decreasing landscape stability. This succession is repeated upsection with a package of mature paleosols overlain by immature paleosols at the top of the unit. Unit III has fewer paleosols with less distinguishable groups. The base of the unit is dominated by gray paleosols; upsection are two apparent periods of enhanced drainage on this landscape marked by packages of red and brown paleosols (separated by a package of gray-red and purple paleosols).

At Fort Mott, the base of Unit II has a package of red and brown paleosols. Upsection, there are multiple gray and purple paleosols indicating decreased drainage conditions interrupted only by a red paleosol near the top. Unit III has repeating packages of red and gray paleosols before the top of the unit is dominated by saturated conditions indicated by multiple purple, gray-red, and gray profiles.

At Medford, fewer paleosols in both units lead to minimal grouping. In Unit II, a singular brown paleosol demonstrates enhanced drainage conditions, indicating increased landscape stability. This brown profile is overlain by gray and gray-red paleosols near the top of the unit, indicating a decrease in landscape stability. Unit III has a group of three paleosols near the unit base that show a trend of increased drainage upsection with a gray paleosol overlain by a gray-red paleosol overlain by a purple paleosol. The only other paleosols in this unit is a group of red and gray-red profiles farther upsection.

Geochemistry

Ba/Sr

Unit I.—Unit I Ba/Sr values are measured only at Fort Mott (Fig. 6), where the lower half of Unit I exhibits generally high values (> 6 excluding 1.4 at 232.9 m), indicating enhanced drainage. The upper half of Unit I at Fort Mott exhibits generally lower (< 4) values, indicating decreased drainage (Fig. 6).

Unit II.—Ba/Sr values measured from Unit II at all three sites are generally low (2–4) (Figs. 6–8, 11; Table 5), indicating less leaching and thus poorer drainage. At Summit Marina (Fig. 7), values are less than 5 except for a value of 7.2 at 105.8 m near the top of the unit. At Fort Mott (Fig. 6), values are generally low throughout (1.3–2.9). At Medford (Fig. 8), values are obtained only from the upper half of this unit and are generally low (1.6–3.4).

Unit III.—Unit III Ba/Sr values show considerable variability at all three sites (Figs. 6–8, 12; Table 5). At Summit Marina and Fort Mott, values range from 2.2 to 5.5 and from 2.1 to 4.2, respectively (Figs. 6, 7).

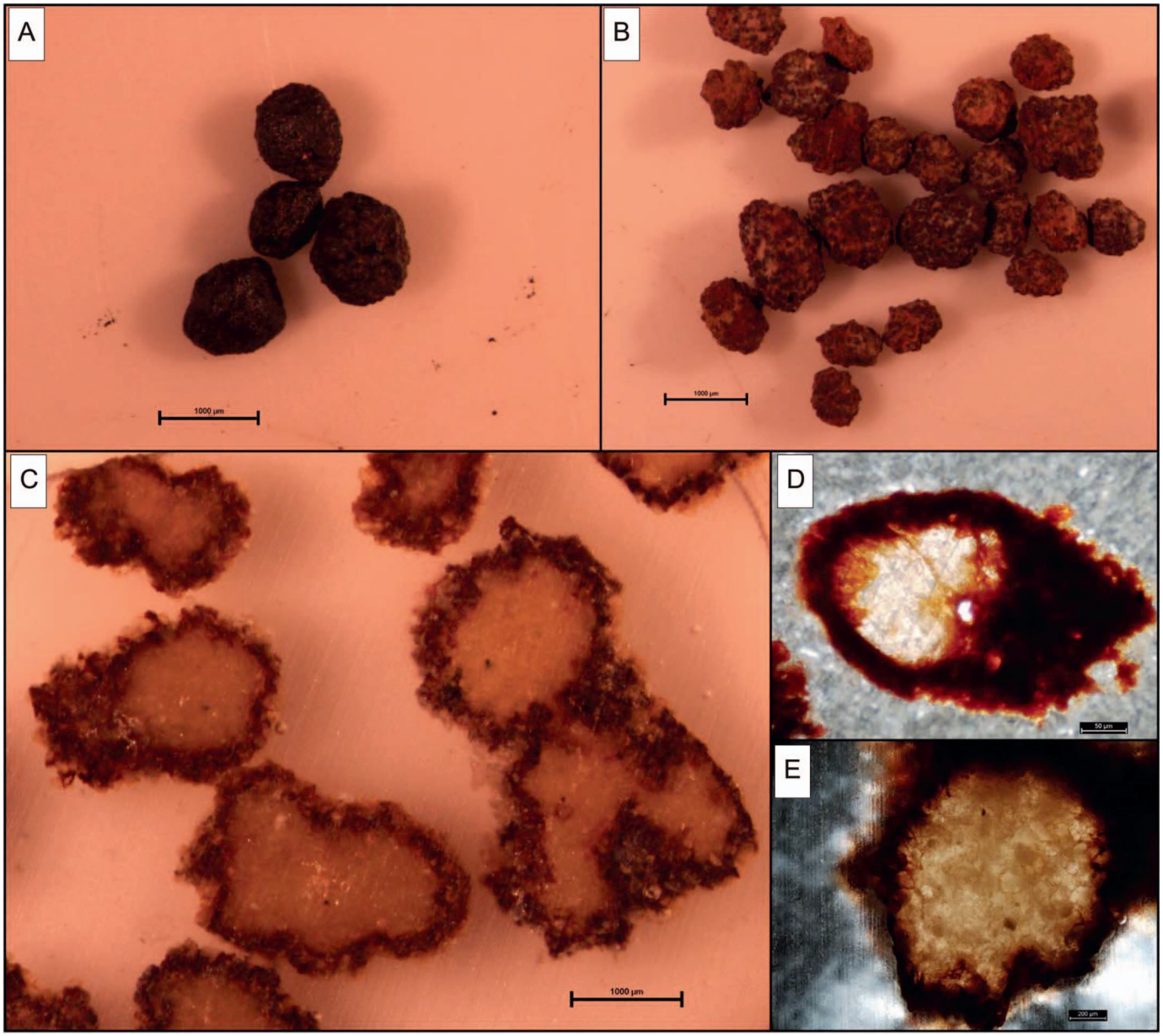

FIG. 9.—Examples of sphaerosiderites: **A)** an example of sphaerosiderites with minimal oxidation; **B)** illustrating oxidization that has occurred on the rind of the sphaerosiderite. Thin-section (Parts C, D, E) image of a sphaerosiderite with oxidation occurring on the rim, **C)** in plane-polar light at 1×, **D)** 20×; **E)** 400× are under cross-polarized light.

At Medford, values were obtained only from the lower half of Unit III and are generally low (1.4–2.9), indicating poor drainage.

$\delta^{18}O_{siderite}$ Data

At Fort Mott $\delta^{18}O_{siderite}$ values from Unit I range from –2.2 to –4.7‰ VPDB, and the calculated $\delta^{18}O_{groundwater}$ values range from –4.2 to –1.7‰ VSMOW (mean –1.0 ± 0.4‰; Fig. 6). In Unit II at Fort Mott, sphaerosiderite $\delta^{18}O_{siderite}$ values range from –1.7 to –2.9‰ VPDB with calculated $\delta^{18}O_{groundwater}$ from –2.5‰ to –1.3‰ VSMOW (mean –2.0 ± 0.4‰; Fig. 6). In Unit III at Fort Mott, $\delta^{18}O_{siderite}$ values range from –3.0‰ to –0.9‰ VPDB and calculated $\delta^{18}O_{groundwater}$ values range from –2.6‰ to –0.4‰ VSMOW (mean –1.6 ± 0.7‰ VSMOW; Fig. 6).

At Summit Marina, Unit II $\delta^{18}O_{siderite}$ values range from –2.5 to –4.6‰ VPDB and calculated $\delta^{18}O_{groundwater}$ values range from –4.2‰ to –2.1‰ VSMOW (mean –3.2 ± 0.7‰; Fig. 7). In Unit III at Summit Marina, $\delta^{18}O_{siderite}$ values that range from –3.7‰ to –1.4‰ VPDB and calculated $\delta^{18}O_{groundwater}$ values range from –5.3‰ to –1.0‰ VSMOW (mean –2.4 ± 1.0‰ VSMOW; Fig. 7).

$\delta^{18}O_{siderite}$ data are sparse at Medford. Unit II values range from –2.5 to 2.9‰ VPDB with calculated $\delta^{18}O_{groundwater}$ values of –4.0 to 4.5‰ VSMOW (mean –4.3 ± 0.1‰; Fig. 8), and Unit III values of –2.5 to –5.2 VPDB with calculated $\delta^{18}O_{groundwater}$ values of –4.1 to –4.8‰ VSMOW (mean –4.4 ± 0.4‰ VSMOW; Fig. 8).

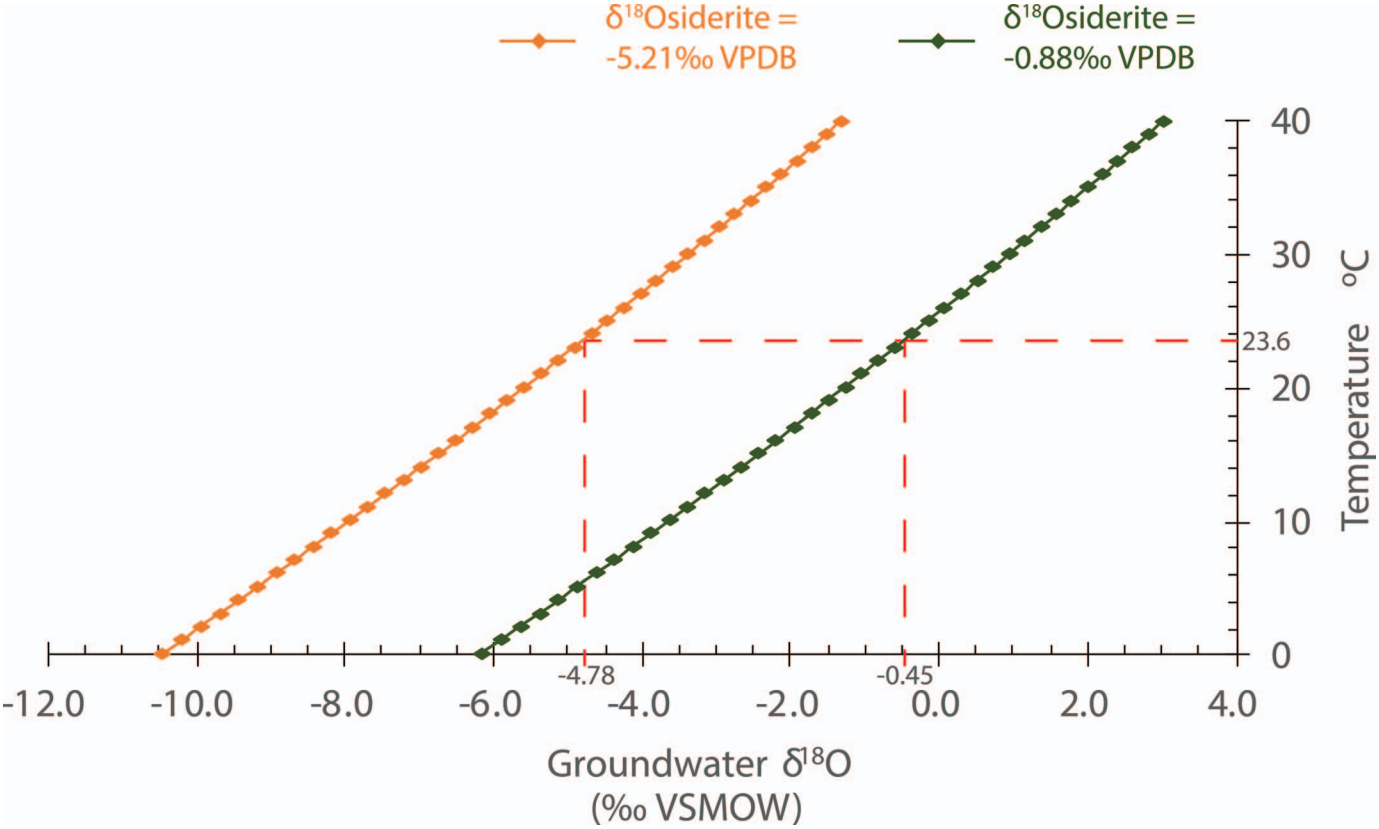

FIG. 10.—Relationship between temperature and $\delta^{18}O$ values. Lines represent the minimum and maximum measured siderite $\delta^{18}O$ values (‰ VPDB) and the calculated groundwater $\delta^{18}O$ values (‰ VSMOW) across a range of temperatures. Red dashed line represents the calculated groundwater $\delta^{18}O$ values for the inferred mid-Cretaceous paleotemperature at these sites during sphaerosiderite formation.

DISCUSSION

Interpretation of Sphaerosiderite Data

The groundwater $\delta^{18}O_{VSMOW}$ values were calculated from measured $\delta^{18}O_{VSMOW}$ values in the pedogenic sphareosiderites. This provides insight into the meteoric paleoprecipitation rates and groundwater interactions during formation, including the interaction of brackish waters from rising base level. White et al. (2005) illustrated that the $\delta^{18}O$ signal produced by the mixing of meteoric and marine waters produce a relationship reflecting less the changes in paleoprecipitation rate and more the changes in base level. This relationship is considered, and the spaherosiderite data are compared with the paleosols to attempt to distinguish climate from base-level interactions.

In Unit III at Fort Mott there is a visual upsection trend towards more positive $\delta^{18}O$ values. This signal likely reflects the increased influence from marine and/or brackish waters, with Cretaceous marine waters having an approximate $\delta^{18}O_{VSMOW}$ value of –1.2‰. An alternative explanation for these positive values would be a decreased precipitation rate during this period. However, the preserved paleosols do not provide any evidence that this is indeed the case. The upsection trend in this unit is towards thinner, immature paleosols exhibiting features of water logging that would be expected during a rise in base level, and the incursion of brackish marine waters into the groundwater system. At both Summit Marina and Medford, the Unit III trends match those at Fort Mott with an upsection move to more positive values. The paleosols and associated sediments at both sites again suggests a likely marine influence from rising base level.

Only at Fort Mott does the Unit II $\delta^{18}O_{VSMOW}$ trend appear similar to Unit III, as it becomes more positive from mid-unit moving upsection towards the unit boundary. This can be interpreted as a move to more marine and/or brackish influence and is associated with a shift to thinner paleosols exhibiting waterlogged conditions, again demonstrating that the $\delta^{18}O_{VSMOW}$ trends cannot be attributed to decreased paleoprecipitation at this site.

Unlike at Fort Mott, both Summit Marina and Medford have visual Unit II $\delta^{18}O_{VSMOW}$ trends with values that are more negative upsection, although, as at Fort Mott, both sites are dominated by thin, immature paleosols exhibiting features of water logging that can be interpreted as a rise in base level. The move towards more negative $\delta^{18}O_{VSMOW}$ values, especially at Summit Marina, may reflect an increased rainfall signal during this period of base-level rise. However, given its proximity to Fort Mott it is unusual to see it recorded in one site but not the other. A potential explanation is that Summit Marina may be positioned closer to an active channel with groundwater exerting less of an influence from potential fluid mixing during base-level rise.

It is noted that the mixing of two distinct fluids can be sometimes be inferred from measured values, as fluid mixing will often produce a variable, hyperbolic curve of oxygen-isotope values. Although we interpret brackish waters having an influence on sphaerosiderite formation, we did not observe any hyperbolic oxygen-isotope curves.

The presence of occasional pyrite is of interest because siderite formation is rare in environments with reduced sulfate (Berner 1984; Driese et al. 2010). In the presence of organic matter and reduced iron, the availability of sulfate becomes the limiting factor in determining the

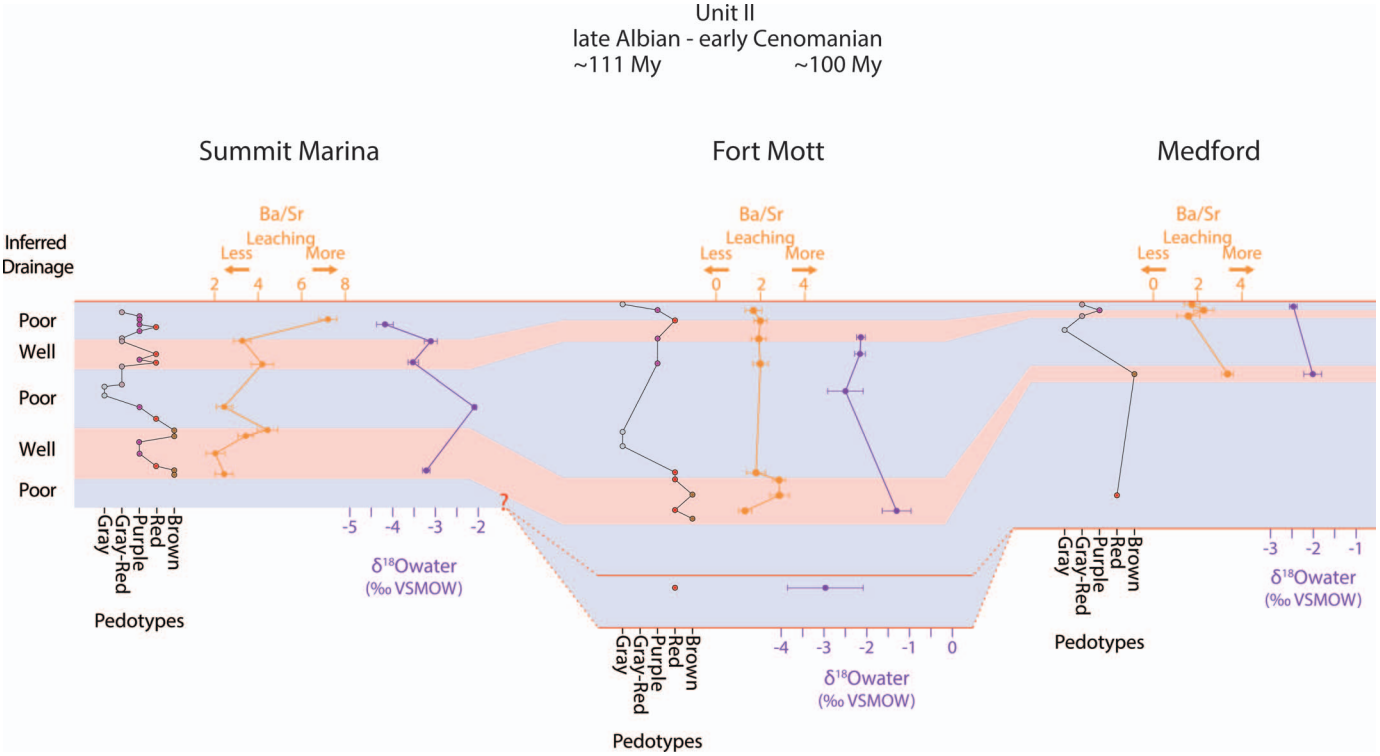

FIG. 11.—Correlation of Unit II among sites at Summit Marina, Fort Mott, and Medford; unit boundaries have been correlated using general lithology as described in the text; correlations within the unit are made on basis of paleosol and proxy trends. Note the Ba/Sr and $\delta^{18}O$ scale differences between sites.

formation of pyrite over siderite (Berner 1984). The possibility exists of pyrite forming from sulfate in a freshwater anaerobic environment in which sulfate-reducing bacteria allow for the anaerobic oxidation of methane (Pye et al. 1990; Ufnar et al. 2001). Once this limited dissolved sulfate has reacted to form pyrite, the result will be the formation of siderite and produce $\delta^{13}C$ values that are increasingly depleted (up to –60‰) (Pye et al. 1990; Ufnar et al. 2001). A second possible pathway for pyrite formation is from the influence of marine porewaters that have

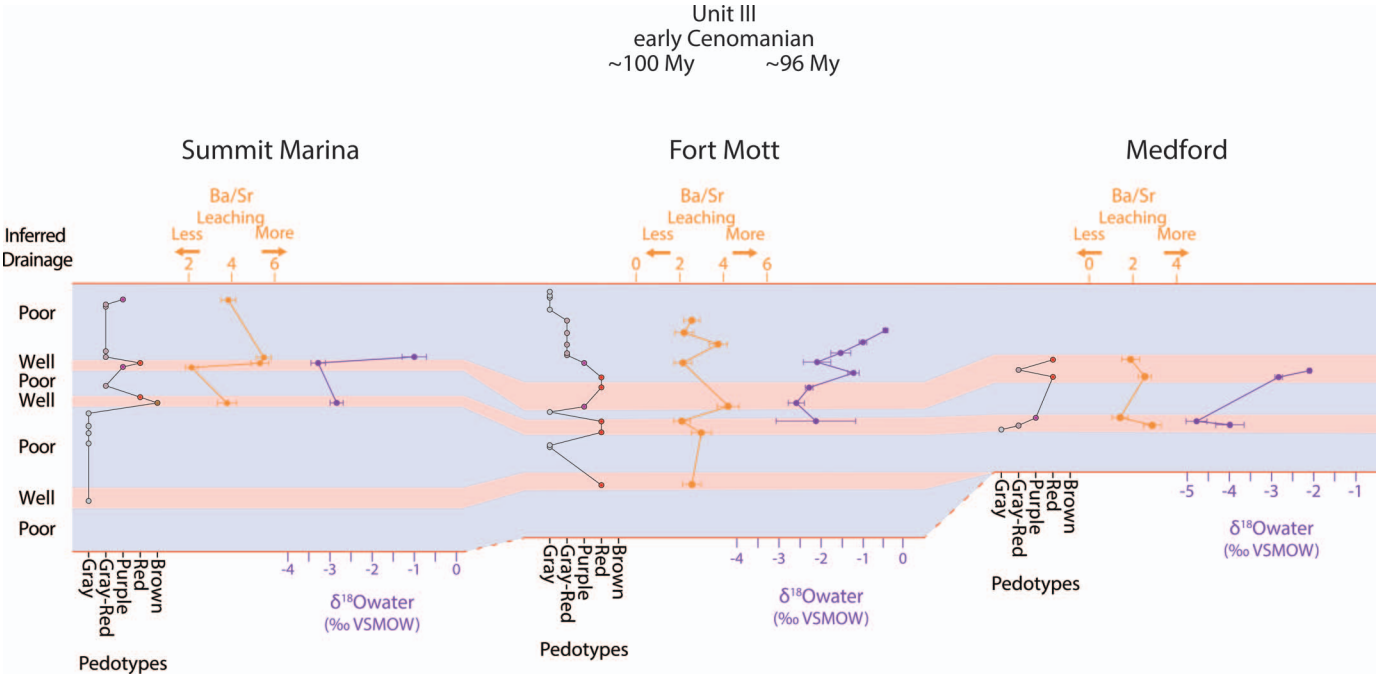

FIG. 12.—Correlation of Unit III among sites at Summit Marina, Fort Mott, and Medford; unit boundaries have been correlated using general lithology as described in the text; correlations within the unit are made on basis of paleosol and proxy trends. Note the Ba/Sr and $\delta^{18}O$ scale differences between sites.

a much higher sulfate concentration. The presence of pyrite and lack of very low $\delta^{13}C$ values in our samples suggests that marginal marine fluid mixing occasionally influenced these sediments (Wright 1986; Pye et al. 1990; Ufnar et al. 2001).

Sphaerosiderite $\delta^{18}O$ values provide insight into meteoric values during their formation. However, the relative proximity of these sites along the coastal plain shows the necessity to consider the influence of rising sea levels resulting in groundwaters that are brackish in nature. Ultimately these sphaerosiderite data aid in the landscape reconstructions interpreted from preserved paleosol deposits.

Landscape Reconstruction

Although the paleosol deposits are generally discontinuous within units, they still provide an overall picture of landscape conditions within and between sites/units. Upsection changes of paleosol maturity within units may reflect shifts in channel positions (Kraus 2002). Changes in paleosol morphology, as opposed to paleosol maturity, reflect changes in the drainage state of the landscape (Platt and Keller 1992; Kraus 2002). When this information from preserved paleosols is compared with proxy data, it allows us to evaluate the importance of base-level changes vs. climate change on this coastal-plain landscape.

We considered the role of evolving flora on landscape evolution. Pollen shows that the evolution of angiosperms was rapid during deposition of the Potomac Formation (Brenner 1963; Doyle and Robbins 1977; Hochuli et al. 2006). However, the effects of angiosperm radiation (Fig. 2) yielded no observable changes in landscape evolution based on comparison of the trends in angiosperm evolution with paleosol type (Thornburg 2016). Rather, the dominant controls on landscape appear to be climate (especially precipitation) and base-level changes.

Unit I Reconstructions.—The base of Unit I at Fort Mott is dominated by multiple mature paleosol profiles (Fig. 6), suggesting an interval with a relatively stable, well-drained landscape. These paleosols reveal landscape conditions that were well-drained (brown type) or with periods of water-table fluctuation (red type). The shift from brown to red type is marked by a decrease in Ba/Sr, suggesting increased precipitation or proximity to a fluvial system caused this shift to a poorly drained landscape.

Overlying this interval and continuing to the top of the unit are stacked purple and red type profiles, occasionally interrupted by sand bodies that suggest that this landscape was periodically waterlogged and occasionally unstable. There is an associated decrease in the Ba/Sr resulting from this decline in drainage condition. Sampled sphaerosiderites produce $\delta^{18}O_{groundwater}$ values that become more negative and likely reflect a shift to increased precipitation during this interval.

Sugarman et al. (2004) has interpreted deposits from Unit I at Fort Mott as representing an anastomosing fluvial system, with the sand bodies representing levee, splay, and channel-fill deposits. Unlike the apparently coeval braided system at Medford, an anastomosing fluvial system has multiple channels, each having good lateral stability, and an overall environment that produces a larger proportion of overbank muds to channel sands (Makaske 2001).

Unit II Reconstructions.—The base of Unit II at Fort Mott contains sands deposited mainly as channel fill, and transitions up-section to brown and red compound paleosols formed on a well-drained, stable landscape (Fig. 6). At Summit Marina, apparently coeval basal sands are overlain by brown, red, and purple compound paleosols (Fig. 7), indicating a similar shift in landscape stability. This apparent abrupt change to a more stable and well-drained landscape is similar to the change noted at Fort Mott. This interpretation of paleosol types is supported by increasing Ba/Sr values in this interval at both sites, corresponding to an increase in drainage conditions on this stable landscape.

Medford has a more ambiguous record at the base of Unit II (Fig. 8). Sand deposits are the most common lithology; less common are interbedded silty–clay deposits and a single red type paleosol. Sugarman et al. (2010) interpreted this sandy interval as fluvial channel fill with interfluvial lacustrine deposits, although we prefer to interpret the base of Unit II at Medford as an unstable landscape with deposition resulting from fluvial avulsion with little to no apparent pedogenic modification. This interpretation is due to the sand deposits that remain relatively coarse, as would be expected from channel flow. There is a single well-drained brown type paleosol overlying these sandy deposits that represents a period of stability on a well-drained landscape.

In the middle part of Unit II at Fort Mott and Summit Marina (Figs. 6, 7), evidence of a stable well-drained landscape gives way upsection to features associated with poorly drained, waterlogged conditions, likely forming on an avulsion belt. Kraus and Aslan (1999) interpreted deposits in an avulsion belt to consist of heterolithic intervals with thin, weakly developed paleosols forming due to the rapid and unsteady nature of deposition during an avulsion. This description fits a generally heterolithic interval at Fort Mott (157.0–129.2 m), including immature gray type paleosols. A similar heterolithic interval is found at Summit Marina (128.0–117.8 m), with a package of weakly developed, immature paleosol profiles. There is a similar trend of immature paleosols preserved at the top of Unit II at Medford. We suggest that this upsection change at these sites is best explained by an increase in avulsion activity resulting from rising base level.

It is also worth noting that the lithofacies present could reflect a marine influence on deposition across this same interval; evidence of this includes very fine to fine sands, heavy-mineral concentrations on bedding planes, and occurrences of pyrite. This shift to more waterlogged conditions with possible marginal marine influences offers a likely correlatable section between Fort Mott and Summit Marina (Fig. 11). A tentative link can be made with these sites to Medford, where cross-bedded, bioturbated fine sands and pyrite is found (257.5–248.7 m) in sediments deposited above a stable, well-drained landscape inferred from a brown type paleosol.

There are similarities among the three sites in the upper part of Unit II where preserved composite and cumulative paleosols are comparable. These profiles are mainly hydromorphic in nature; however, there appears an upsection period of some increased landscape stability, including better profile development with enhanced relative drainage.

Continuing upsection, approaching the Unit II boundary at each site, there are weakly developed gray and gray-red compound paleosols forming under generally waterlogged conditions. This change in landscape stability generally agrees with the Ba/Sr values suggesting decreased drainage. Summit Marina exhibits a transition from a waterlogged, unstable surface (gray and gray-red type) to a more stable surface with periodic fluctuations of the water table (purple and red type) before again shifting back to waterlogged, saturated conditions at the top of the unit. This is likely an artifact of local landscape positioning with respect to the fluvial system, as the maturity of the paleosol profile is related to the lateral distance to the channel. As mentioned above, the difference in $\delta^{18}O_{VSMOW}$ values between Fort Mott and Summit Marina is noted. Although the paleosol packages at both sites are similar, reflecting the similarity in landscape conditions, the thinner compound paleosols preserved at Summit Marina may reflect a position closer to a main fluvial channel whose fresh-water influence on groundwater would mask brackish-marine mixing in the $\delta^{18}O_{VSMOW}$ values. This would explain the $\delta^{18}O$ discrepancy without changing the overall interpretation made from preserved paleosol deposits.

Unit III Reconstructions.—As in Unit II, there is an interval of sand at the base of Unit III at all three sites (Figs. 6–8), interpreted to be a generally waterlogged, unstable landscape with only minor periods of pedogenesis. At Fort Mott, there is an upsection package of red and purple paleosols that mark a period of increased landscape stability. Similarly, at

Summit Marina and Medford, packages of mature, well-drained paleosols mark a period of prolonged landscape stability. Geochemical evidence points to enhanced drainage, agreeing with this assessment of landscape stability.

At the top of Unit III, at all three sites, landscape instability returns as evidenced by packages of sands and silts with either preserved paleosols that were immature and poorly drained or sediments exhibiting little to no pedogenic features. In this interval, decreased Ba/Sr values indicate poor drainage, and when coupled with the more positive $\delta^{18}O$ values indicate a likely influence from brackish groundwater pointing to rising base level as the cause of this waterlogged landscape.

Correlation

The use of preserved paleosol profiles coupled with two geochemical proxies allow the reconstruction of paleolandscapes through the mid-Cretaceous, with base level inferred to be the main driver on regional landscape stability through Units II and III. These trends in landscape stability and drainage conditions are used to correlate Units II and III across these three sites (Figs. 11, 12).

Further correlation of these sites in a global context are considered here. The rise in base level inferred in Unit II and III may indicate transgressive events during this period and can be potentially correlated to major sea-level rises occurring in the late Albian and early Cenomanian (Glaser 1969; Haq 2014).

Lower in Unit II, well-drained, well-developed red and brown paleosols transition upsection to heterolithic sand deposits with poorly developed, thin gray paleosols. This transition is likely the result of increased avulsions due to rising base level and can potentially be correlated with the major sea-level rise of the late Albian (Haq 2014). Similar to the upper part of Unit II, there is an upsection trend to the top of Unit III with increasingly waterlogged, poorly developed, thin paleosols that represent deposition during a base-level rise resulting from a transgression. This interval can be potentially correlated to the major rise in sea level during the early Cenomanian (Haq 2014).

The type of paleosol deposited is a response to landscape conditions, and changes in the landscape are manifested in the group or packages of preserved paleosols. These packages can be tied to changes in base level and are used here to tentatively create correlation surfaces. However, further refinement of these paleosol packages is needed to definitively link to these global sea-level events.

White et al. (2005) noted that the Albian–Cenomanian boundary along the Western Interior Seaway was marked by a large negative $\delta^{18}O$ excursion in sphaerosiderite data, and when taken with an associated paleosol profile is inferred to represent the Albian–Cenomanian lowstand. This boundary would likely fall within upper reaches of Unit II, although no large negative trend in $\delta^{18}O$ is found at any site in this study. The lack of a negative trend is partially due to inadequate material near the unit tops that precludes sampling to confirm the reported excursion along the eastern margin of North America during this interval. A possible exception is at Summit Marina near the top of Unit II (106.7 m), where $\delta^{18}O$ values trend more negative. This sample location is directly above a single red paleosol in a package of gray-red and purple paleosols; a similar package of paleosols is found at Fort Mott, and this period of enhanced drainage is possibly associated with a fall in base level due to a lowstand. Thus, this package series serves as a possible correlation surface tied to sites along the Western Interior Seaway margin, although further refinement is again needed to definitively place the Albian–Cenomanian boundary here (Figs. 7, 11).

CONCLUSIONS

We analyzed Potomac Formation paleosols from two sites in New Jersey (Fort Mott and Medford) and one in Delaware (Summit Marina) to understand the landscape evolution along part of the eastern margin of North America during the transition from Early to Late Cretaceous (Aptian–Albian–Cenomanian). An analysis of morphological features, both micro- and macro-, allows these paleosols to be grouped into five general pedotypes. These range in pedogenic maturity from weakly developed, poorly drained, Inceptisol-like gray and gray-red paleosols, to moderately developed, Alfisol-like, hydromorphic purple and red paleosols, and well developed, well-drained, Alfisol-like brown paleosols.

Two geochemical proxies (Ba/Sr and $\delta^{18}O$ of pedogenic sphaerosiderites) were applied to aid in this landscape reconstruction. All were in generally good agreement with interpretations made using the paleosol profile morphology and maturity. These proxies provide information on paleodrainage (Ba/Sr) and paleoprecipitation and/or paleogroundwater (sphaerosiderites); this allows the cause of landscape conditions to be estimated, from a rise or fall in base level to a change, increase or decrease, in precipitation. Unit I is inferred from Fort Mott to have a relatively well-drained and stable landscape compared with Units II and III. These Units (II and III) are inferred from all three sites to have more instability dominated by poorly drained landscape conditions, although there are limited episodes of stability and enhanced drainage conditions.

Paleosols and associated proxies allow these interpretations of surface conditions and emphasized the role that base level and climate (paleoprecipitation) have on paleosol formation. Evaluation of these paleosols and proxy trends also reveal intervals of similar surface conditions persisting for extended periods; these intervals offer correlatable surfaces, especially if these surface conditions are the result of the same inferred influence (base level vs. precipitation).

Unit I is recovered at Fort Mott and Medford, with deposition occurring on a river dominated landscape. The basal sands at Fort Mott were deposited by an anastomosing river system, whereas apparent coeval sands at Medford were deposited by a braided river system. Paleosols at Fort Mott and their relevant proxies provide evidence that the landscape underwent two alternating intervals of drainage conditions that were controlled mainly by changes in precipitation.

Unit II is recovered at all three sites, with deposition occurring on an anastomosing river delta-plain. Paleosols and proxies at all three sites indicate two main intervals of alternating drainage conditions influencing landscape development. The proxies indicate the major role of base-level change driving these conditions, although not singularly responsible, with all sites showing periods of landscape influence driven by precipitation. Correlations were made between these sites using these intervals of poorly drained and well-drained landscape conditions.

Unit III is recovered at all three sites, with deposition occurring on a river-dominated delta plain. Paleosols and proxies at all three sites indicate three alternating intervals of drainage conditions before an interval of saturated, waterlogged conditions dominate in the uppermost portion of the unit. As in Unit II, these conditions are driven largely by changes in base level, although several periods appear to be influenced by precipitation changes. Correlations are again made using these intervals of landscape similarity.

SUPPLEMENTAL MATERIAL

Supplemental files are available from JSR's Data Archive: https://www.sepm.org/pages.aspx?pageid=229.

ACKNOWLEDGMENTS

This study was part of a Ph.D. Thesis at Rutgers University supported by the Department of Earth and Planetary Sciences. Samples were provided by International Ocean Discovery Program. We thank P.J. Sugarman and P.P. McLaughlin for comments and Nicholas Davatzes and George Myer for help with the analyses. Support was from National Science Foundation grant

OCE14-63759 (to K. Miller). Insightful reviews by associate editor G. Ludvigson, T. White, and an anonymous reviewer were helpful.

REFERENCES

Barron, E.J., 1983, A warm, equable Cretaceous: the nature of the problem: Earth-Science Reviews, v. 19, p. 305–338.

Barron, E.J., 1987, Cretaceous Plate Tectonic Reconstructions: Palaeogeography, Palaeoclimatology, Palaeoecology, v. 59, p. 3–29.

Benson, R.N., and McLaughlin, P.P., 2006, Internal stratigraphic correlation of the subsurface Potomac Formation, New Castle County, Delaware, and adjacent areas in Maryland and New Jersey: Delaware Geological Survey, Report of Investigations, v. 71, 15 p.

Berner, R.A., 1984, Sedimentary pyrite formation: an update: Geochimica et Cosmochimica Acta, v. 48, p. 605–615.

Berner, R.A., 2006, GEOCARBSULF: a combined model for Phanerozoic atmospheric O_2 and CO_2: Geochimica et Cosmochimica Acta, v. 70, p. 5653–5664.

Berner, R.A., 2009, Phanerozoic atmospheric oxygen: new results using the GEOCARBSULF model: American Journal of Science, v. 309, p. 603–606.

Brenner, G.J., 1963, The spores and pollen of the Potomac Group of Maryland: Maryland Department of Geology, Mines, and Water Resources, Bulletin 27, 215 p.

Brewer, R., 1964, Fabric and Mineral Analysis of Soils: New York, John Wiley and Sons, 470 p.

Browning, J.V., Miller, K.G., Sugarman, P.J., Kominz, M.A., McLaughlin, P.P., Jr., Kulpecz, A.A., and Feigenson, M.D., 2008, 100 Myr record of sequences, sedimentary facies and sea-level change from Ocean Drilling Program onshore coreholes, US Mid-Atlantic coastal plain: Basin Research, v. 20, p. 227–248.

Cerling, T.E., 1984, The stable isotopic composition of modern soil carbonate and its relationship to climate: Earth and Planetary Science Letters, v. 71, p. 229–240.

Doyle J.A., and Hickey L.J., 1976, Pollen and leaves from the Mid-Cretaceous Potomac group and their bearing on early angiosperm evolution, *in* Beck, C.B., ed., Original and Early Evolution of Angiosperms: New York, Columbia University Press, p. 139–206.

Doyle, J.A., and Robbins, E.I., 1977, Angiosperm pollen zonation of the continental Cretaceous of the Atlantic Coastal Plain and its application to deep wells in the Salisbury Embayment: Palynology, v. 1, p. 43–78.

Driese, S.G., Ludvigson, G.A., Roberts, J.A., Fowle, D.A., González, L.A., Smith, J.J., Vulava, V.M., and McKay, L.D., 2010, Micromorphology and stable-isotope geochemistry of historical pedogenic siderite formed in PAH-contaminated alluvial clay soils, Tennessee, USA: Journal of Sedimentary Research, v. 80, p. 943–954.

Dworkin, S.I., Nordt, L., and Atchley, S., 2005, Determining terrestrial paleotemperatures using the oxygen isotopic composition of pedogenic carbonate: Earth and Planetary Science Letters, v. 237, p. 56–68.

Fitzpatrick, E.A., 1993, Soil Microscopy and Micromorphology: Chichester, UK, John Wiley and Sons, 304 p.

Francis, J.E., and Frakes, L.A., 1993, Cretaceous Climates, *in* Wright, V.P., ed., Sedimentology Review: Oxford, UK, Blackwell Publishing, p. 17–30.

Glaser, J.D., 1969, Petrology and origin of Potomac and Magothy (Cretaceous) sediments, Middle Atlantic Coastal Plain: Maryland Geological Survey, Report of Investigations, no. 11, 102 p.

Gradstein, F.M., Ogg, J.G., Schmitz, M., and Ogg, G., 2012, The Geologic Time Scale 2012, v. 1–2: Oxford, UK, Elsevier, 1176 p.

Hansen, H.J., and Doyle, J.A., 1982, Hydrogeologic framework and potential utilization of the brine aquifers of the Waste Gate Formation, a new unit of the Potomac Group underlying the Delmarva Peninsula, pt. 1: Waste Gate Formation: Maryland Department of Natural Resources, Geological Survey, Open-File Report 82-02.

Haq, B.U., 2014, Cretaceous eustasy revisited: Global and Planetary Change, v. 113, p. 44–58.

Hay, W.W., DeConto, R.M., Wold, C.N., Wilson, K.M., Voigt, S., Schulz, M., Wold-Rossby, A., Dullo, W.C., Ronov, A.B., Balukhovsky, A.N., and Söding, E., 1999, Alternative global Cretaceous paleogeography, *in* Barrera, E., and Johnson, C.C., eds., Evolution of the Cretaceous Ocean–Climate System: Geological Society of America, Special Paper 332, p. 1–47.

Hickey, L.J., and Doyle, J.A., 1977, Early Cretaceous fossil evidence for angiosperm evolution: The Botanical Review, v. 43, p. 3–104.

Hochuli, P.A., Heimhofer, U., and Weissert, H., 2006, Timing of early angiosperm radiation: recalibrating the classical succession: Geological Society of London, Journal, v. 163, p. 1–8.

Jenny, H., 1941, Factors of Soil Formation, First Edition: New York, McGraw-Hill, 281 p.

Kominz, M.A., Browning, J.V., Miller, K.G., Sugarman, P.J., Mizintseva, S., and Scotese, C.R., 2008, Late Cretaceous to Miocene sea-level estimates from the New Jersey and Delaware coastal plain coreholes: an error analysis: Basin Research, v. 20, p. 211–226.

Kraus, M.J., 1999, Paleosols in clastic sedimentary rocks: their geologic applications: Earth-Science Reviews, v. 47, p. 41–70.

Kraus, M.J., 2002, Basin-scale changes in floodplain paleosols: implications for interpreting alluvial architecture: Journal of Sedimentary Research, v. 72, p. 500–509.

Kraus, M.J., and Aslan, A., 1999, Palaeosol sequences in floodplain environments: a hierarchical approach, *in* Thiry, M., Simon-Coinçon, R., Kraus, M.J., and Aslan, A., eds., Palaeoweathering, Palaeosurfaces, and Related Continental Deposits, p. 303–321.

Landuyt, C.J., 1990, Micromorphology of iron minerals from bog ores of the Belgian Campine area, *in* Douglas, L.A., ed., Soil Micromophology: A Basic and Applied Science: Amsterdam, Elsevier, Developments in Soil Science, v. 19, p. 289–294.

Lidgard, S., and Crane, P.R., 1988, Quantitative analyses of the early angiosperm radiation: Nature, v. 331, p. 344–346.

Ludvigson, G.A., González, L.A., Metzger, R.A., Witzke, B.J., Brenner, R.L., Murillo, A.P., and White, T.S., 1998, Meteoric sphaerosiderite lines and their use for paleohydrology and paleoclimatology: Geology, v. 26, p. 1039–1042.

Ludvigson, G.A., González, L.A., Fowle, D.A., Roberts, J.A., Driese, S.G., Villarreal, M.A., Smith, J.J., and Suarez, M.B., 2013, Paleoclimatic applications and modern process studies of pedogenic siderite, *in* Driese, S.G., Nordt, L.C., eds., New Frontiers in Paleopedology and Terrestrial Paleoclimatology: Paleosols and Soil Surface Analog Systems: SEPM, Special Publication 104, p. 79–87.

Mack, G.H., James, W.C., and Monger, H.C., 1993, Classification of paleosols: Geological Society of America, Bulletin, v. 105, p. 129–136.

Makaske, B., 2001, Anastomosing rivers: a review of their classification, origin and sedimentary products: Earth-Science Reviews, v. 53, p. 149–196.

Miller, K.G., Kominz, M.A., Browning, J.V., Wright, J.D., Mountain, G.S., Katz, M.E., Sugarman, P.J., Cramer, B.S., Christie-Blick, N., and Pekar, S.F., 2005, The Phanerozoic record of global sea-level change: Science, v. 310, p. 1293–1298.

Miller, K.G., Browning, J.V., Sugarman, Monteverde, D.H., Andreasen, D.C., Lombardi, C., Thornburg, J.D., Fan, Y., and Kopp, R.E., 2017, Lower to mid-Cretaceous sequence stratigraphy and characterization of CO_2 storage potential in the Mid-Atlantic U.S. Coastal Plain: Journal of Sedimentary Research, v. 87, p. 609–629. doi:10.2110/jsr.2017.33

Mitchum, R.M., Jr., Vail, P.R., and Thompson, S., III, 1977, Seismic stratigraphy and global changes of sea level: Part 2, The depositional sequence as a basic unit for stratigraphic analysis, *in* Payton, C.E., ed., Seismic Stratigraphy: Applications to Hydrocarbon Exploration: American Association of Petroleum Geologists, Memoir 26, p. 53–62.

Moore, D.M., and Reynolds, R.C., 1997, X-Ray Diffraction and the Identification and Analysis of Clay Minerals: Oxford, UK, Oxford University Press, 378 p.

Mora, C.I., Driese, S.G., and Colarusso, L.A., 1996, Middle to late Paleozoic atmospheric CO_2 levels from soil carbonate and organic matter: Science, v. 271, p. 1105–1107.

Munsell, 2000, Munsell Soil Color Charts: New Windsor, NY, Gretag Macbeth.

Nordt, L., Orosz, M., Driese, S., and Tubbs, J., 2006, Vertisol carbonate properties in relation to mean annual precipitation: implications for paleoprecipitation estimates: The Journal of Geology, v. 114, p. 501–510.

Norris, R.D., Bice, K.L., Magno, E.A., and Wilson, P.A., 2002, Jiggling the tropical thermostat in the Cretaceous hothouse: Geology, v. 30, p. 299–302.

Olsson, R.K., Gibson, T.G., Hansen, H.J., and Owens, J.P., 1988, Geology of the northern Atlantic Coastal Plain: Long Island to Virginia, *in* Sheridan, R.E., and Grow, J.A., eds., The Atlantic Coastal Margin, U.S.: Geological Society of America, The Geology of North America, v. 1–2, p. 87–105.

Platt, N.H., and Keller, B., 1992, Distal alluvial deposits in a foreland basin setting: the Lower Freshwater Molasse (Lower Miocene), Switzerland: sedimentology, architecture and palaeosols: Sedimentology, v. 39, p. 545–565.

Poulsen, C.J., 1999, The mid-Cretaceous ocean circulation and its impact on greenhouse climate dynamics [Ph.D. thesis]: University Park, Pennsylvania State University, 219 p.

Pye, K., Dickson, J.A.D., Schiavon, N., Coleman, M.L., and Cox, M., 1990, Formation of siderite–Mg–calcite–iron sulphide concretions in intertidal marsh and sandflat sediments, north Norfolk, England: Sedimentology, v. 37, p. 325–343.

Retallack, G.J., 1994, A pedotype approach to latest Cretaceous and earliest Tertiary paleosols in eastern Montana: Geological Society of American, Bulletin, v. 106, p. 1377–1397.

Retallack, G.J., 2001, Soils of the Past: An Introduction to Paleopedology, Second Edition: London, Blackwell Science, 404 p.

Royer, D.L., Berner, R.A., Montanez, I.P., Tabor, N.J., and Beerling, D.J., 2004, CO_2 as a primary driver of Phanerozoic climate change: GSA Today, v. 14, n. 3, p. 4–10.

Schaetzl, R.J., and Anderson, S., 2005, Genesis and Geomorphology: Cambridge, UK, Cambridge University Press, 827 p.

Schoeneberger, P.J., Wysocki, D.A., Benham, E.C., and Broderson, W.D., eds., 2002, Field book for describing and sampling soils, Version 2.0.: Lincoln, Nebraska, Natural Resources Conservation Service, National Soil Survey Center.

Scotese, C.R., Gahagan, L.M., and Larson, R.L., 1988, Plate tectonic reconstructions of the Cretaceous and Cenozoic ocean basins (in Mesozoic and Cenozoic plate reconstructions): Tectonophysics, v. 155, p. 27–48.

Sheldon, N.D., and Retallack, G.J., 2001, Equation for compaction of paleosols due to burial: Geology, v. 29, p. 247–250.

Sheldon, N.D., and Tabor, N.J., 2009, Quantitative paleoenvironmental and paleoclimatic reconstruction using paleosols: Earth-Science Reviews, v. 98, p. 1–52.

Soil Survey Staff, 1999, Soil Taxonomy: A Basic System of Soil Classification for Making and Interpreting Soil Surveys, Second Edition: Natural Resources Conservation Service, U.S. Department of Agriculture, Handbook 436.

Spicer, R.A., and Corfield, R.M., 1992, Phanerozoic atmospheric CO_2 change: evaluating geochemical and paleobiological approaches: Geological Magazine, v. 129, no. 2, p. 169–180.

Stoops, G., 1983, SEM and light microscopic observations of minerals in bog-ores of the Belgian Campine: Amsterdam, Elsevier, Developments in Soil Science, v. 12, p. 179–186.

Suarez, M.B., González, L.A., and Ludvigson, G.A., 2011, Quantification of a greenhouse hydrologic cycle from equatorial to polar latitudes: The mid-Cretaceous water bearer revisited: Palaeogeography, Palaeoclimatology, Palaeoecology, v. 307, p. 301–312.

Sugarman, P.J. , Miller, K.G., McLaughlin, P.P., Jr., Browning, J.V., Hernandez, J., Monteverde, D.H., Uptegrove, J., Bazter, S.J., Mckenna, T.E., Andres, A.S., Benson, R.N., Ramsey, K.W., Keyser, T., Katz, M.E., Kahn, A., Friedman, A., Wojtko, M., Feigenson, M.D., Olsson, R.K., Brenner, G., Self-Trail, J.M., and Cobbs, G., III, 2004, Fort Mott site, *in* Miller, K.G., Sugarman, P.J., Browning, J.V., et al., eds., Proceedings of the Ocean Drilling Program, Initial Reports, v. 174X (Suppl.), p. 1–50.

Sugarman, P.J., Miller, K.G., Browning, J.V., Kulpecz, A.A., McLaughlin, P.P., Jr., and Monteverde, D.H., 2005, Hydrostratigraphy of the New Jersey Coastal Plain: sequences and facies predict continuity of aquifers and confining units: Stratigraphy, v. 2, p. 259–275.

Sugarman, P.J., Miller, K.G., Browning, J.V., Aubry, M.-P., Brenner, G.J., Bukry, D., Butari, B., Feigenson, M.D., Kulpecz, A.A., McLaughlin, P.P., Jr., Mizintseva, S., Monteverde, D.H., Olsson, R., Pusz, A.E., Rancan, H., Tomlinson, J., Uptegrove, J., and Velez, C.C., 2010, Medford site *in* Miller, K.G., Sugarman, P.J., Browning, J.V., et al., eds., Proceedings of the Ocean Drilling Program, Initial Reports, 174AX (Suppl.), p. 1–93.

Thornburg, J.D., 2016, Reconstructing landscapes across the early to late Cretaceous transition: evaluating base level, climate and sequence stratigraphy from Potomac Formation sediments in New Jersey and Delaware [Ph.D. thesis]: Rutgers University, 246 p.

Ufnar, D.F., González, L.A., Ludvigson, G.A., Brenner, R.L., and Witzke, B.J., 2001, Stratigraphic implications of meteoric sphaerosiderite ^{18}O values in paleosols of the Cretaceous (Albian) Boulder Creek Formation, NE British Columbia Foothills, Canada: Journal of Sedimentary Research, v. 71, p. 1017–1028.

Ufnar, D.F., González, L.A., Ludvigson, G.A., Brenner, R.L., and Witzke, B.J., 2002, The mid-Cretaceous water bearer: isotope mass balance quantification of the Albian hydrologic cycle: Palaeogeography, Palaeoclimatology, Palaeoecology, v. 188, p. 51–71.

Ufnar, D.F., González, L.A., Ludvigson, G.A., Brenner, R.L., and Witzke, B.J., 2004, Evidence for increased latent heat transport during the Cretaceous (Albian) greenhouse warming: Geology, v. 32, p. 1049–1052.

Ufnar, D.F., Ludvigson, G.A., González, L.A., and Gröcke, D.R., 2008, Precipitation rates and atmospheric heat transport during the Cenomanian greenhouse warming in North America: estimates from a stable isotope mass-balance model: Palaeogeography, Palaeoclimatology, Palaeoecology, v. 266, p. 28–38.

van Dijk, J., Fernandez, A., Müller, I.A., Lever, M., and Bernasconi, S.M., 2018, Oxygen isotope fractionation in the siderite–water system between 8.5 and 62°C: Geochimica et Cosmochimica Acta, v. 220, p. 535–551.

White, T.S., González, L.A., Ludvigson, G.A., and Poulsen, C.J., 2001, Middle Cretaceous greenhouse hydrologic cycle of North America: Geology, v. 29, p. 363–366.

White, T., Witzke, B., Ludvigson, G., and Brenner, R., 2005, Distinguishing base-level change and climate signals in a Cretaceous alluvial sequence: Geology, v. 33, p. 13–16.

Wright, V.P., 1986, Pyrite formation and the drowning of a palaeosol: Geological Journal, v. 21, p. 139–149.

Wolfe, J.A., and Upchurch, G.R., 1987, Leaf assemblages across the Cretaceous–Tertiary boundary in the Raton Basin, New Mexico and Colorado: National Academy of Sciences (USA), Proceedings, v. 84, p. 5096–5100.

Zullo, C.C., 2012, Seismic imaging and hydrogeologic characterization of the Potomac Formation in Northern New Castle County, Delaware [Ph.D. thesis]: Newark, University of Delaware, 218 p.

Received 9 February 2018; accepted 7 January 2019.